Water mass age and dissolved organic matter properties drive the diversity of pelagic prokaryotes in the Western Mediterranean Sea

Grazia Marina Quero [a,b,*], Simona Retelletti Brogi [c,d], Chiara Santinelli [b,c], Gian Marco Luna [a,b]

[a] Institute for Biological Resources and Marine Biotechnologies, National Research Council (IRBIM-CNR), Largo Fiera della Pesca 2, 60125, Ancona, Italy
[b] National Biodiversity Future Center (NBFC), 90133, Palermo, Italy
[c] Biophysics Institute, National Research Council (IBF-CNR), Via G. Moruzzi, Pisa, 56124, Italy
[d] Istituto di Oceanografia e Geofisica Sperimentale (OGS) - Sezione di Oceanografia, Borgo Grotta Gigante 42/C, Sgonico, TS, 34010, Italy

ABSTRACT

The deep sea is among the largest, yet still poorly known, ecosystems on Earth. This knowledge gap is particularly evident for the bathypelagic layer (between 1000 and 4000 m) of the deep Mediterranean Sea (MS), characterized by peculiar environmental conditions at meso- and bathypelagic depths, such as the thermal signature of the deep waters, showing temperatures approximately 10 °C higher than any oceanic system at comparable depths. This sustains high rates of prokaryotic activities and fast dissolved organic matter (DOM) mineralization rates, and likely selects for unique microbial assemblages. We collected seawater samples in stations representative of different areas of the Western Mediterranean Sea (Algero-Provençal Basin, Alboran Sea and Gulf of Lion), from the surface to the bathypelagic layer (down to 2680 m) and in different water masses, and described the composition of pelagic prokaryotic communities, along with measurements of the main physical-chemical variables, concentration and optical properties (absorption and fluorescence) of DOM. Remarkable differences in DOM optical properties were observed among water masses, with highest dissolved organic carbon (DOC) values in surface waters and lowest in the oldest water masses represented by the Western Mediterranean Deep Water (WMDW) and the Levantine Intermediate Water (LIW), which were characterized by the highest concentration of recalcitrant DOM. The water mass had a significant partitioning effect on microbial community composition, which showed the highest richness in LIW. DOC, the marine humic-like component of DOM (C_{1mh}) and oxygen were the main drivers of prokaryotic community structure. Changes in quality of DOM were reflected in shifts in community composition, supporting the existence of strong relationships between DOM quality and microbial community composition in the deep MS. Our data shed light on the community composition and diversity patterns of prokaryotic plankton in the deep western MS, helping to elucidate the major microbial players in the DOM cycling, and to progress towards a better comprehension of its future trends in light of changing conditions that are modifying the oceanography of the entire MS basin.

1. Introduction

The Mediterranean Sea (MS) is the largest semi-enclosed basin on Earth (Coll et al., 2010; Siokou-Frangou et al., 2010), and is recognized as a hot-spot for future climatic changes (Giorgi, 2006), where significant modifications, including changes in the thermohaline circulation and the carbon cycle, can be observed on scales of human lifetime (Schroeder et al., 2016). The basin features unique geomorphological, geological, hydrological and biogeochemical characteristics influencing marine biodiversity (Álvarez et al., 2023). One of the main distinctive features of the MS is the thermal signature of the deep waters, characterized by warm temperatures (typically 12.5–13 °C also at abyssal depths), approximately 10 °C higher than any oceanic system at comparable depths, which sustain high rates of prokaryotic activities and faster dissolved organic matter (DOM) mineralization rates compared to other deep ocean basins (Santinelli et al., 2010; Luna et al., 2012; Santinelli 2015; Rahav et al., 2019).

Marine DOM is the largest ocean reservoir of reduced carbon, holding >200 times the carbon inventory of marine biomass (Hansell 2013). DOM plays a crucial role in the functioning of the microbial food

web, representing the main source of energy for the microbial community. The assimilated DOM is used by heterotrophic prokaryotes for both biomass synthesis, i.e. cell growth and replication, and respiration. The balance between these two processes can have profound impacts on the global carbon cycle, leading to carbon sequestration or CO_2 production and, ultimately, playing a key role in controlling the Earth's climate. Despite its importance, understanding the relationship between DOM dynamics (concentration and quality) and the microbial community remains a challenge (LaBrie et al., 2021). For instance, one of the most intriguing question in chemical oceanography is why DOM persists in the oceans for millennia and what is the role of microbial diversity in driving this feature (Dittmar et al., 2021). Deep ocean microbial communities are astoundingly versatile and metabolically flexible in utilizing DOM, and recent experimental studies have suggested they have a higher ability to process DOM than surface microbes, likely explained by the recruitment of a comparatively larger number of opportunistic taxa within the bathypelagic assemblages resulting in a broader community capability of substrate utilization (Sebastián et al., 2021a). Microbial diversity and DOM dynamics are undoubtedly related and influence each other, but the extent of this relationship in deep waters is still far from being completely elucidated.

In the MS, DOM shows concentration and distribution comparable to those observed in the oceans, with a clear role of water mass circulation in DOM transport and distribution in the basin (Santinelli et al., 2010, 2012, 2013, 2015, 2021). DOM mineralization has been studied following the core of the Levantine Intermediate Water (LIW), suggesting that 38–49% of oxygen consumption is due to DOM mineralization during its route from the Levantine Basin to the Tyrrhenian Sea (Santinelli et al., 2010, 2012). Interestingly, in the intermediate and deep waters of the MS, DOC concentrations are equal to the lowest values found in the deep Atlantic and Pacific oceans, however radiocarbon data indicate that DOM in the MS is approximately 1000 years older than in the oceans (Santinelli et al., 2015). Thus, due to its peculiarities and the occurrence of similar processes driving DOM distribution, the MS has been suggested as a natural laboratory for the study of DOC dynamics and bacterioplankton/organic matter interactions in the deep sea.

Although microbes are the key players in the ecosystem functioning and global biogeochemical cycles in the deep sea (Arístegui et al., 2009; Burd et al., 2010), our knowledge on microbial diversity in the dark ocean, its patterns and drivers, and the metabolic and genetic inventory of the unicellular organisms is still rudimentary (Mende et al., 2017). This holds especially true for MS bacterioplankton diversity and community structure, for which studies have been made available only starting in recent years (reviewed in Luna, 2015). Besides pioneer studies carried by cultivation or targeting specific bacteria (Giuliano et al., 1999; López-López et al., 2005), the diversity of meso- or bathypelagic bacterioplankton communities in the MS has been studied only at specific locations, such as the Southern Adriatic Sea (Korlević et al., 2015; Luna et al., 2016), the Ligurian Sea (Celussi et al., 2018), the Tyhrrenian Sea (Tamburini et al., 2009), the North Western MS (Severin et al., 2016; Mestre et al., 2017) and the Eastern MS (De Corte et al., 2009). Martín-Cuadrado et al. (2007) provided the first metagenomics-based survey in one sample from the bathypelagic MS (Ionian Sea), reporting dominance of metabolic genes related to catabolism, transport and degradation of complex organic molecules suggesting a prevalent heterotrophic lifestyle. Mapelli et al. (2013) used a fingerprinting technique to study patterns of diversity across the whole MS, reporting shifts in community composition according to several variables that included longitude, depth, temperature and salinity. Only recently, Sebastián et al. (2021b) performed the first comprehensive quasi-synoptic investigation at the basin-scale, providing evidence that environmental gradients and physical barriers drive the basin-wide spatial structuring of MS planktonic microbes. Despite these studies, the identity of prokaryotes in the intermediate and deep waters of the MS, as well as the patterns and the environmental drivers of their diversity, remain still scarcely investigated, leaving unresolved important

questions about the identity of the major ecological players of the basin and how DOC dynamics relate to changes in diversity.

In this study, we studied prokaryoplankton diversity, community composition and DOM dynamics in 3 basins of the Western MS (the Gulf of Lion, the Algero-Provençal Basin and the Alboran Sea), characterized by different trophic regimes. Differently to previous studies that focused on differences between Western and Eastern basins and the main drivers in the different basins, our study focuses on the main water masses occurring in different sub-basins of the Western MS from the surface to the bathypelagic layer, to test the hypothesis that microbial assemblages vary in the different water masses, and that they are significantly structured by the quantity and quality of DOM.

2. Materials and methods

2.1. Study site and sampling strategy

Samples were collected during the oceanographic cruise WBMED 2014 from April 10th to 23rd 2014 on board the CNR oceanographic vessel Urania. Seawater samples were collected in Niskin bottles at 5 stations located (i) in the Alboran Sea (ST034 and ST036), (ii) the Algero-Provençal Basin (ST019), and (iii) the Gulf of Lion (ST054 and ST060) (Fig. 1, Table S1). The sampling depths were chosen by looking at the vertical profiles of physical parameters, in order to collect samples in the core of the different water masses.

Measurements for conductivity, pressure, temperature, dissolved oxygen and chlorophyll *a* (Chl a) were performed using a CTD-rosette system, that included a CTD SBE 911 *plus* probe complemented with an oxygen sensor and a fluorometer and a General Oceanic sampler with 24 Niskin bottles. Data were processed in real time, visualized and corrected to eliminate errors. Apparent Oxygen Utilization (AOU) was calculated as follows:

AOU = Oxygen at saturation – dissolved oxygen

2.2. DOM analysis

Samples for DOC, CDOM and FDOM analysis were collected in dark glass bottles, preconditioned with filtered, open seawater and rinsed 3 times with the sample before its collection. Samples were filtered on board through sterile 0.2 μm nylon filters (Sartorius, 17845 ACK) under low pressure. Filtered samples were stored in amber glass bottles at 4 °C in the dark until the analysis. DOC measurements were carried out with a Shimadzu TOC-Vcsn Analyzer, following the method reported by Santinelli et al. (2015). The instrument performance was verified by comparison with DOC Consensus Reference Waters (CRM) (Hansell 2005) (CRM Batch #08–13 nominal concentration of 41–44 μM; measured concentration 42.1 ± 1.2 μM).

Samples for CDOM and FDOM were brought at room temperature before analysis. Absorbance spectra were measured between 230 and 700 nm using a UV-visible spectrophotometer (Jasco Mod-7850) equipped with a 10 cm quartz cuvette, following the method reported by Retelletti Brogi et al. (2015) and elaborated using the ASFit tool (Omanović et al., 2019). The absorption coefficient at 254 (a_{254}) was calculated as an indicator of CDOM concentration (Del Vecchio and Blough, 2004). The spectral slope between 275 and 295 nm ($S_{275-295}$) was calculated to gain information on changes in DOM properties since its value is inversely related to the average molecular weight and aromaticity of the molecules (Helms et al., 2008). Fluorescence excitation-emission Matrixes (EEMs) were obtained using the Aqualog spectrofluorometer (Horiba). Excitation ranged between 250 and 450 nm at 5 nm increment, emission was recorded between 212 and 620 nm every 3 nm. The EEMs were subtracted by the EEM of Milli-Q water, and the TreatEEM software (Omanović Dario, TreatEEM—program fo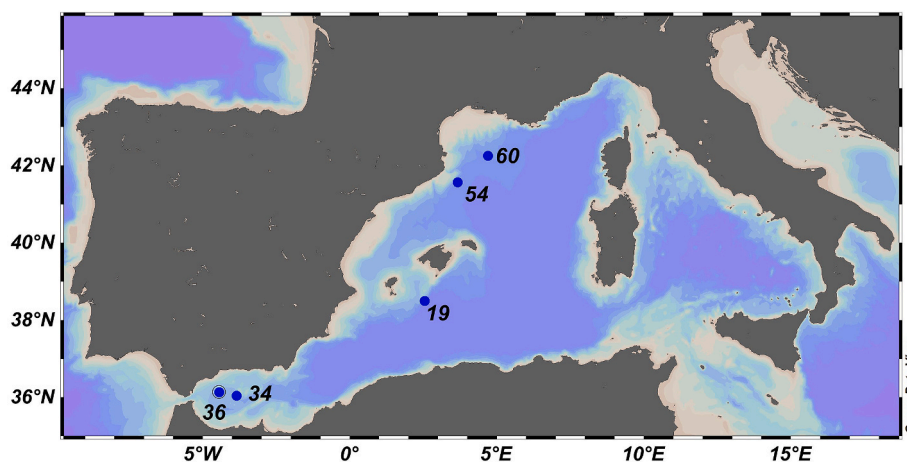r treatment of fluorescence excitation-emission matrices, https://sites.google.com/site/daromasoft/home/treateem) was used to remove

Fig. 1. Map of the study area with indication of the sampling stations. The map has been created using the ODV software (https://odv.awi.de/).

Rayleigh and Raman scatter peaks, and to normalize to Raman Units (R. U.). PARAllel FACtor analysis (PARAFAC, drEEM Toolbox, Murphy et al., 2013) was carried out, and the validation of the PARAFAC model was performed by visual inspection of the residuals, split-half analysis and percentage of explained variance (97.8%). The analysis resulted in the validation of a 3-component model (Fig. S1, Table S2). The 3 components were characterized by comparison with the OpenFluor database (Murphy et al., 2014) (Table S2). C1 was characterized as marine humic-like (C1$_{mh}$), C2 as terrestrial humic-like (C2$_{th}$), C3 as protein-like (C3$_p$).

2.3. DNA extraction, PCR, sequencing and data analysis

Molecular analyses were performed on samples listed in Table S2. DNA extraction was performed by using the PowerWater DNA Isolation Kit (MoBio Laboratories, California) on 0.2 μm cellulose nitrate filters (Sartorius) after filtration of 2 L of seawater. The manufacturer's instructions were followed with few modifications to increase the DNA yield and quality, as described in Quero et al. (2017). These included two additional vortexing steps (following the one that is recommended by the manufacturer) at the maximum speed for 2 min, each one being preceded by an incubation step at 70 °C for 5 min, and with the addition of one more washing step with Solution C5 as an additional removal step for contaminants. The concentration of each DNA extract was determined using a Qubit Fluorometer (Thermo-Fisher), and the DNA was then stored at 80 °C until PCR. Illumina Miseq sequencing analyses were carried out on the hypervariable V3 and V4 regions of the 16S rRNA gene by amplifying using the 341F (5′-CCTACGGGNGGCWGCAG-3′) and 785R (5′-GACTACHVGGGTATCTAATCC-3′) universal bacterial primers (Eiler et al., 2012), using V3 chemistry (2 X 300 bp). Paired-end reads were quality checked (with default settings and minimum quality score of 20) and analyzed with QIIME v1.8.0 software package (Quantitative Insights Into Microbial Ecology) (Caporaso et al., 2010). Reads were clustered into OTUs operational taxonomic units) using UCLUST v1.2.22 (Edgar, 2010) with a >97% similarity threshold with an open-reference OTU picking strategy and default settings. Chimeras were detected using USEARCH v6.1 (Edgar, 2010). Chimera checking and taxonomy assignment were performed using Silva 138 as reference database (https://www.arb-silva. de/documentation/release-138/). The OTU table was then rarefied to an even number of sequences per sample to ensure an equal sampling depth for all samples (n = 17,461). All sequences have been submitted to the SRA Sequence Read Archive (BioProject Accession No. PRJNA649377).

2.4. Data analyses

Rarefaction curves of observed OTUs based on the subsampled OTU table were calculated in R Studio (package *vegan*). Alpha-diversity indices were calculated with the R package *BiodiversityR* (Kindt and Coe, 2005). Non-metric multiDimensional Scaling (nMDS) was performed using the *metaMDS* function based on a Bray–Curtis dissimilarity matrix, using an OTU table modified by the *autotransform* option. The presence of significant differences in community composition between areas and water masses was assessed in R environment using the analysis of similarity (ANOSIM) tool, based on a Bray–Curtis similarity matrix. Multivariate, multiple regression analyses were performed to identify drivers (among temperature, salinity, density, dissolved oxygen, chlA [as resulting from fluorometric measurements], DOC, CDOM [a$_{254}$], C1$_{mh}$, C2$_{th}$, C3$_p$) of prokaryotic community composition in the investigated samples. The analysis was performed using PERMANOVA through the *bioenv* approach (*vegan* package). Selected variables were used to perform Canonical Correspondence Analysis (CCA). A heatmap was constructed using OTUs with greater than 1% as their maximum relative abundance in our dataset and plotted with *ComplexHeatmap* (Gu, 2016). A correlogram of the OTUs most represented in the different water masses with environmental variable was calculated and plotted with *corrplot* (Wei and Simko, 2021). All analyses were performed in RStudio environment (RStudio Team, 2015).

3. Results

3.1. Water masses

Potential temperature/salinity (θ/S) diagrams allowed for the identification of the main water masses present in the study area. At stations 34 and 36, the Atlantic Water (S < 37; θ = 16–17 °C), entering the MS through the Gibraltar Strait, occupied the surface layer (AW, Fig. 2a). At station 19, the surface layer was characterized by the presence of the Modified Atlantic Water (MAW, Fig. 2a). The higher salinity of MAW (S > 37.5), with respect to the AW, indicates that this water has been circulating in the MS, undergoing evaporation and mixing with the MS waters. At stations 54 and 60, the surface layer displayed the coldest (θ < 16 °C) and saltiest (38 < S<38.5) water. These characteristics, together with the very low stratification of the water column (Fig. S2), suggest the occurrence of a recent upwelling of intermediate waters leading to the mixing of the upper water column. These surface samples are hereinafter indicated as UPW. The upwelling is further supported by the Chl-a surface maxima (Table 1), which can be attributed to a phytoplankton bloom stimulated by the upwelled nutrient-rich waters.

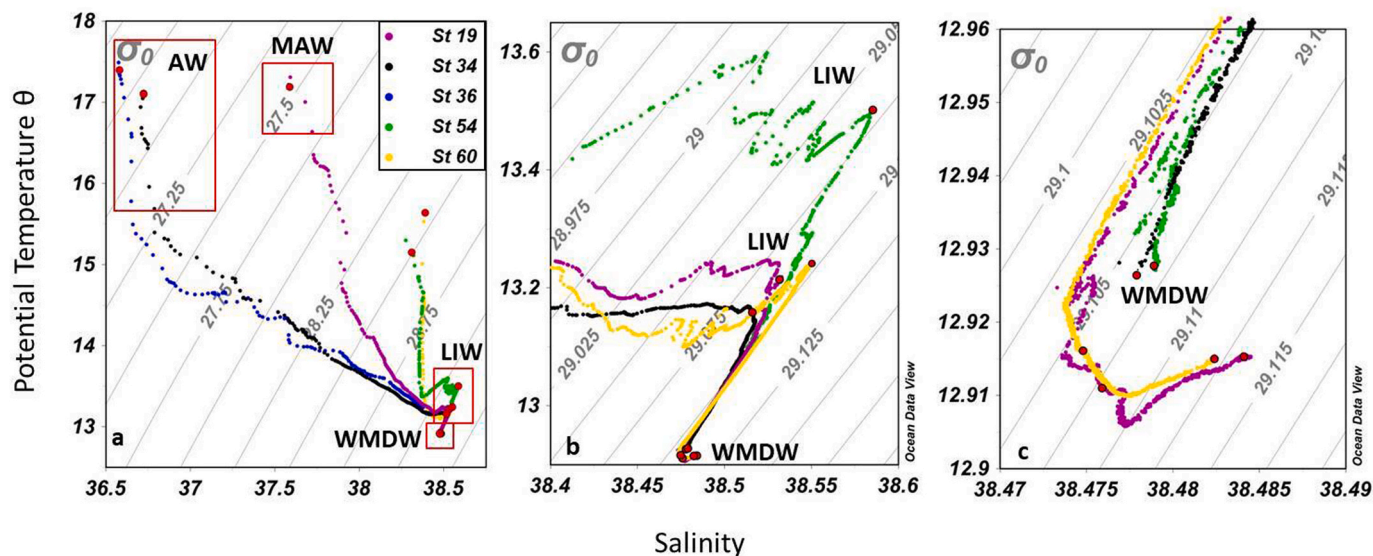In the intermediate layer, the samples were collected in the core of

Fig. 2. θ/S diagram for the 5 sampled stations (a); zoom of the intermediate and deep waters (b); zoom of the deep waters (c). The identified water masses are indicated on the plots. Red dots refer to the depths where samples were collected. AW: Atlantic Water; MAW: Modified Atlantic Water; LIW: Levantine Intermediate Water; WMDW: West Mediterranean Deep Water.

Table 1
Physico-chemical and DOM properties of the samples collected in the different water masses.

Sample	Station	Depth (m)	T (°C)	Salinity	Oxygen (μM)	AOU (μM)	Chl-a (U. Fl.A)	DOC (μM)	a_{254} (m^{-1})	$S_{275-295}$ (nm^{-1})	$C1_{mh}$ (R. U.)	$C2_{th}$ (R. U.)	$C3_p$ (R. U.)
Surface													
ST_019_SUP	19	0	17.19	37.59	247		0.089	60.4	1.45	0.034	0.0132	0.0032	0.0161
ST_034_SUP	34	0	17.10	36.72	259		0.152	57.3	1.21	0.031	0.0124	0.0030	0.0136
ST_036_SUP	36	0	17.49	36.58	256		0.056	54.1	1.24	0.036	0.0157	0.0067	0.0105
ST_054_SUP	54	0	15.30	38.28	258		0.333	57.2	1.31	0.031	0.0176	0.0075	0.0098
ST_060_SUP	60	0	15.64	38.39	264		0.503	54.8	1.26	0.029	0.0175	0.0083	0.0093
Levantine Intermediate Water (LIW)													
ST_019_370	19	370	13.27	38.53	178	78		43.0	0.86	0.029	0.0207	0.0051	0.0111
ST_034_400	34	400	13.22	38.52	171	84		43.5	0.92	0.026	0.0216	0.0061	0.0093
ST_054_230	54	230	13.54	38.59	176	78		45.5	0.88	0.033	0.0190	0.0076	0.0091
ST_060_420	60	420	13.30	38.55	181	75		43.6	0.83	0.027	0.0188	0.0072	0.0119
Western Mediterranean Deep Water (WMDW)													
ST_019_1500	19	1500	13.14	38.48	194	64		42.1	0.94	0.025	0.0195	0.0050	0.0142
ST_019_2680	19	2680	13.33	38.48	196	62		43.1	0.89	0.026	0.0188	0.0047	0.0136
ST_034_1238	34	1238	13.11	38.48	187	70		44.3	0.88	0.027	0.0219	0.0060	0.0163
ST_054_1441	54	1441	13.14	38.48	192	65		43.1	0.83	0.030	0.0126	0.0076	0.0029
ST_060_1500	60	1500	13.14	38.48	192	65		42.4	0.73	0.032	0.0161	0.0073	0.0062
ST_060_2100	60	2100	13.24	38.48	195	62		42.5	0.76	0.032	0.0159	0.0066	0.0100

the Levantine Intermediate Water (LIW) at all the stations, as indicated by their salinity maximum (Fig. 2b). At ST54 the highest salinity (S > 38.55) was observed, suggesting the occurrence of the less eroded and well-defined LIW core. At the other stations an eroded, yet still evident, core of the LIW was observed (S = 38.52–38.55). The marked difference in salinity maximum between stations 54 and 60 may be attributed to a higher extent of vertical mixing at station 60 than 54, reducing the salinity values in the LIW core. This observation is further supported by the highest oxygen concentration (Table 1, Fig. S3) observed in the LIW at station 60. It is noteworthy that, at all the stations, the core of the LIW was characterized by an oxygen minimum (Fig. S3), supporting previous observations that, at these stations, LIW represents the oldest water mass (Santinelli et al., 2010, 2015).

At all the stations, the deep waters were characterized by the presence of the Western Mediterranean Deep Water (WMDW, Fig. 2c).

3.2. DOM dynamics in the different water masses

In the surface waters, DOC showed the highest concentration,

ranging from 54.1 to 60.4 μM (average 56.8 ± 2.5 μM, Table 1) and showing an inverse linear relationship with the Chl-a. This relationship may be driven by the upwelling of LIW (rich in nutrients and poor in DOC) in the Gulf of Lion, which stimulated the phytoplankton growth (high Chl-a). A remarkable difference in DOM optical properties was observed among the stations located in the Alboran Sea and those in the Gulf of Lion, that is between AW and MAW. In the MAW, both the humic-like components were higher, whereas C_P and $S_{275-295}$ were lower than in the AW. These data indicate a different DOM quality in the two water masses, further supporting the effect of the upwelling. DOM in the LIW is characterized by higher humic-like fluorescence and, on average, bigger and more aromatic molecules than in the surface layer (Table 1). Thus, the LIW upwelling would increase humic-like fluorescence and molecular complexity of surface samples as well as decrease DOC concentration. A decrease in $S_{275-295}$ in correspondence with the Chl-a maximum has been observed previously (Galletti et al., 2019). The upwelling of the old, DOC-poor LIW and its mixing with surface water is a possible explanation of the observed differences in DOC and CDOM. However, we cannot exclude that the phytoplankton bloom, producing

labile DOM, may have stimulated the microbial activity enhancing the consumption of the surface DOM, and that the DOM released by phytoplankton is richer in humic-like substances and more complex. It is noteworthy that ST_036 showed a completely different dynamic of DOM with respect to the other stations (Table 1). Here, the minima of both Chl-a and DOC, the maximum of $S_{275-295}$ and intermediate values of the fluorescence components were observed (Table 1). These differences, especially in comparison with ST_034, are very difficult to explain and would deserve further investigation. The area close to the Gibraltar Strait is very complex and vertical mixing could be relevant, making strong spatial gradients. These differences might be partially attributed to the higher influence of AW at ST_36, as suggested by the slightly lower salinity observed in the surface sample with respect to ST_34 (Fig. 2A, Fig. S2, Table 1).

In the LIW, DOC concentrations were very low and did not change significantly among stations (average 43.9 ± 1 μM, Table 1), suggesting that almost all the semi-labile DOC had been already removed by microbial activity. Following the decrease in oxygen, and therefore the ageing of the water, we found an increase in a_{254} and $C1_{mh}$, while $C3_p$ decreased, indicating a change in DOM quality with the ageing of LIW.

In the deep layers, the oldest vein (oxygen = 187 μM) of the WMDW was observed at station 34. Similar values of oxygen (192–196 μM; AOU = 62-56 μM) were observed in the Gulf of Lion (St. 54 and 60) and in the Alboran Sea (St.19), indicating no veins of recently ventilated WMDW at these stations. This observation is in agreement with the very low DOC values observed at depth (42–44 μM) (Table 1). Indeed, other authors observed that, in recently ventilated WMDW (AOU = 45 ± 2 μM), DOC was 52 ± 4 μM, whereas in the old veins (AOU >60 μM), DOC was about 42 μM (Santinelli et al., 2010) as observed in our study.

Looking at the entire water column, $C1_{mh}$ showed its maximum fluorescence in the LIW at all the stations, that is in the oldest water mass observed in the study area, supporting the occurrence of a more reworked and recalcitrant DOM in LIW. These results are in agreement with Martínez-Pérez et al. (2019), which showed molecular weight, oxygenation and degradation index increasing with the ageing of water masses and DOM reworking in the MS.

3.3. Prokaryotic diversity and community composition

After quality trimming and chimera removal, the complete 16S rDNA dataset comprised 849,025 reads from the 15 analyzed samples with, on average, 56,600 reads per sample, for a total of 7800 prokaryotic OTUs detected. After normalization of the dataset at 17,461 reads per sample, a total of 5239 OTUs were obtained. Rarefaction curves based on the normalized dataset (Fig. S4) highlighted that the sequencing effort applied was sufficient to describe the whole prokaryotic diversity.

Despite the primers used in this study target mostly Bacteria while not providing a representative picture of the whole archaeal assemblages, it is worth mentioning that we found from 0.27 to 15.73% per sample of archaeal sequences, particularly abundant in LIW water samples. These taxa were thus included in our further analyses. OTU richness ranged, in each sample, from 498 (ST_36_SUP) to 1454 (ST_19_370) OTUs (Fig. S5-A). Overall, richness values were found to be significantly different among water masses (Kruskal–Wallis, p = 0.02564). An increasing trend in richness from surface (i.e., AW, MAW and the upwelled waters in ST54 and ST60, UPW, avg. 576 ± 60 OTUs) to LIW (avg. 1327 ± 169 OTUs) samples was observed (Fig. S2-A). WMDW samples displayed also higher richness values than the surface samples (avg. 1029 ± 227 OTUs), although these values were lower than those in the LIW. Shannon and Pielou's Evenness indices indicated a similar trend (Fig. S5-A). When comparing alpha-diversity indices among water masses in each sampled area, we found that, in general, the same trend was observed when taking into account values of richness. Conversely, Shannon diversity highlighted an increasing diversity of prokaryotic communities with depth, with the exception of the Gulf of Lion, where WMDW showed a lower diversity than LIW (Fig. S5-B).

Similarly, evenness showed a general increasing trend with increasing depth (Fig. S5-B).

NMDS ordination based on the OTU composition showed that the sampled microbial communities could be distinguished on the basis of their taxonomic differences and according to depth (Fig. 3A). However, surface samples at Alboran Sea stations separated from those from the Gulf of Lion and Algero-Provençal Basin; LIW and WMDW samples clustered based on NMDS1 axis, grouping according to the water mass.

The water mass partitioning effect was statistically supported by the ANOSIM analysis (R = 0.482; p = 0.012). Relative abundances of major prokaryotic taxa varied with depth and water mass (Fig. 3B). In all samples, the phylum Proteobacteria was the most represented (on average, 36.45%). Within this phylum, the classes Alphaproteobacteria (average 21.4%), Gammaproteobacteria (average 15%) were the most abundant. Within Alphaproteobacteria, SAR11 clade represented the most abundant taxon, accounting for 1.8–25.3% of total communities and showing the highest abundances (on avg., 16.32%) in LIW samples at all stations (Fig. S6). Gammaproteobacteria increased with depth, although LIW and WMDW displayed comparable relative abundances in this taxon. In surface waters, Cyanobacteria and Bacteroidota were also among the most abundant classes observed, especially in the Gulf of Lion. Cyanobacteria included almost exclusively the genus *Synechococcus*, which represented in surface samples 3.4–38.4% of the total community, showing the highest abundances in the Gulf of Lion (26.8–38.4% of the total community) and in the Algero-Provençal Basin (35.5% of the total community) (Fig. S7). Chloroflexi, Marinimicrobia (SAR406 clade) and Planctomycetota increased with depth, with the last two phyla showing average higher values in LIW than in WMDW. Deep Gulf of Lion samples were also particularly enriched in Firmicutes. Relative abundances of Thermoplasmatota were higher in LIW and WMDW than in surface waters, with highest values observed in LIW samples. Overall, Archaea represented about 7.9% of the total dataset, with maximum values observed in mesopelagic ST_019_370 (Algero-Provençal Basin; 15.7%).

3.4. Drivers of prokaryotic diversity

PERMANOVA (plotted in CCA; Fig. S8) showed that DOC, dissolved oxygen and $C1_{mh}$ constituted the set of variables most significantly explaining the microbial community composition in our samples. Together, these parameters explained 32.25% of the taxonomic variance between samples. In particular, CCA showed that the physico-chemical parameters structured the samples first along an axis separating surface and deep samples (CCA1), with surface samples being strongly related to dissolved oxygen and DOC. As for the NMDS ordinations (Fig. 3A), samples belonging to the same water depth were generally well separated by the first two CCA axes. Also, LIW and WMDW samples separated along CCA2 axis, although ST_034_1238 appeared to cluster more closely to LIW samples than to the WMDW communities. Moreover, within the surface group, samples separated along CCA2 according to the sampling area. $C1_{mh}$ appeared to be mainly and strongly related to LIW and, to a lesser extent, to WMDW.

3.5. Most abundant OTUs and their relationship with the environmental variables

Over the entire dataset, members of *Synechococcus* (35.6%, observed almost exclusively in surface samples), *Thermoanaerobacter* (14.6%), Flavobacteriaceae (NS4 marine group) (10.10%), archaeal Marine group II (14%), *Alteromonas* (7.7%), *Soehngenia* (6.9%), Thioglobaceae (SUP05 cluster) (6.2%) and the alphaproteobacterial AEGEAN-169 marine group (4.5%) represented the 10 top OTUs. More in detail, surface and deep water masses were characterized by different sets of most abundant microbes (Fig. 4). In surface water masses (AW, MAW and UPW), a clear cluster of OTUs was easily identified as being abundant almost exclusively in these masses. Conversely, deep water masses shared part of the
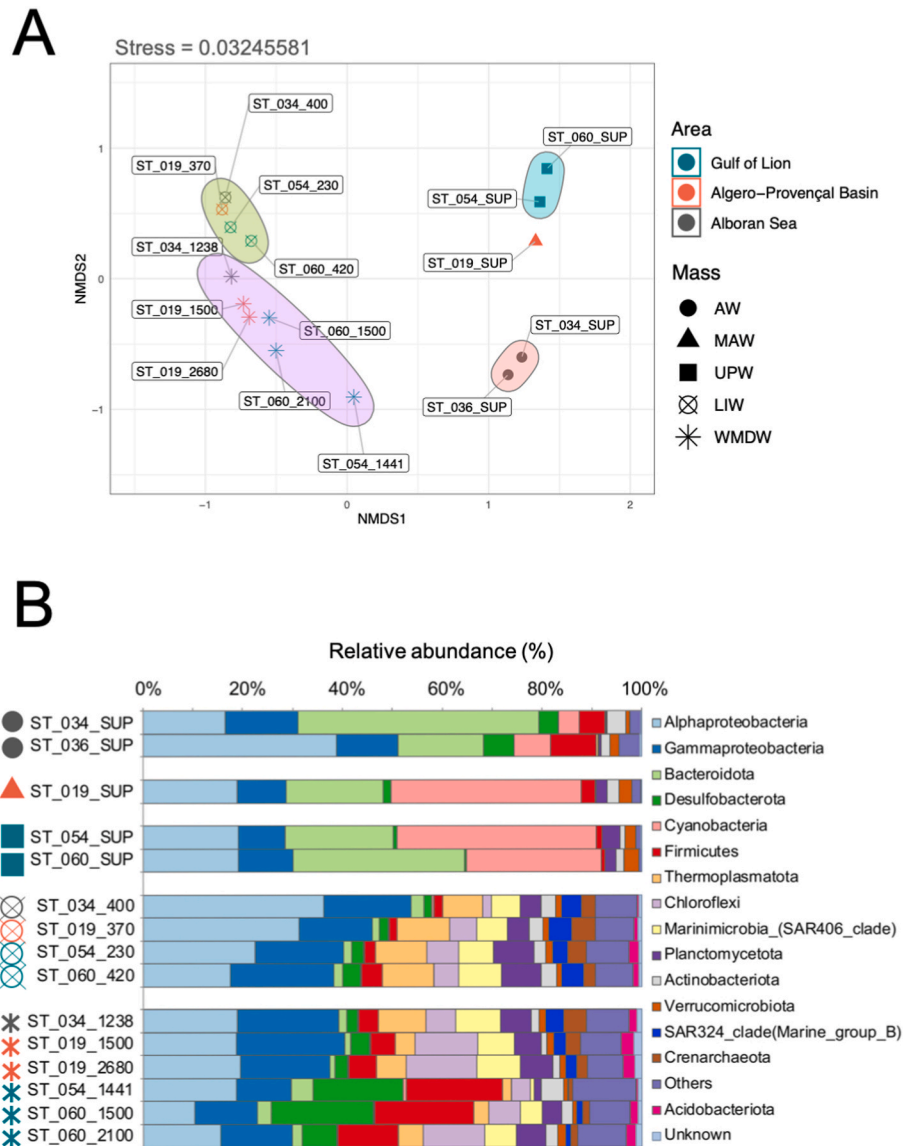
Fig. 3. A) NMDS of prokaryotic communities based on the Bray–Curtis dissimilarity matrix. B) relative abundance of prokaryotic phyla, or classes (for Proteobacteria), in the different samples according to water mass. Phyla or classes showing a mean relative abundance across all samples <1% were aggregated into the group reported as "Others".

most abundant OTUs, although at different extents in LIW and WMDW (Fig. 4).

The abundant taxa in surface waters were mainly represented by *Synechococcus*, Flavobacteriaceae (NS4 marine group), *Thermoanaerobacter*, the gammaproteobacterial OM60 (NOR5) clade and *Amylibacter*. Correlation analyses (represented in the correlogram in Fig. 5) highlighted that most of surface taxa were significantly and positively correlated with temperature, oxygen, Chl-a, DOC and a_{254}, with a general negative correlation with salinity and light.

In the deep Mediterranean Sea (LIW and WMDW), the most abundant OTUs included *Thermoanaerobacter*, the archaeal Marine Group II, *Alteromonas*, *Soehngenia*, the gammaproteobacterial SUP05 cluster, the alphaproteobacterial AEGEAN-169 marine group and SAR324 and 406 clades. Deep sea (LIW and WMDW) OTUs (Fig. 5) displayed significant positive correlations with salinity and $C1_{mh}$, whereas negative correlations were observed in relation to temperature, oxygen, DOC and a_{254}. Overall, bathypelagic OTUs showed scarcity of significant correlations with the measured environmental parameters.

4. Discussion

Marine microbial communities are well known to differ between water masses and depths (Agogué et al., 2011; Dobal-Amador et al., 2016), with deep water masses acting as bio-oceanographic islands for bacterioplankton (Agogué et al., 2011). It is also known that DOM dynamics in the MS are strongly affected by water masses origin, age and circulation (Santinelli et al., 2010, 2013; Santinelli 2015). Resource availability for microbial metabolism typically changes drastically along the water column, with higher DOC concentrations present in the productive surface layer, where it is produced, while deep waters are nutrient-rich but limited by the decreasing availability of easily metabolizable organic carbon (Sebastián et al., 2021a and references therein). All these features were confirmed in our study, where microbial communities showed a marked separation according to the water mass, with a higher dissimilarity between surface and deep samples (LIW and WMDW) than between LIW and WMDW.
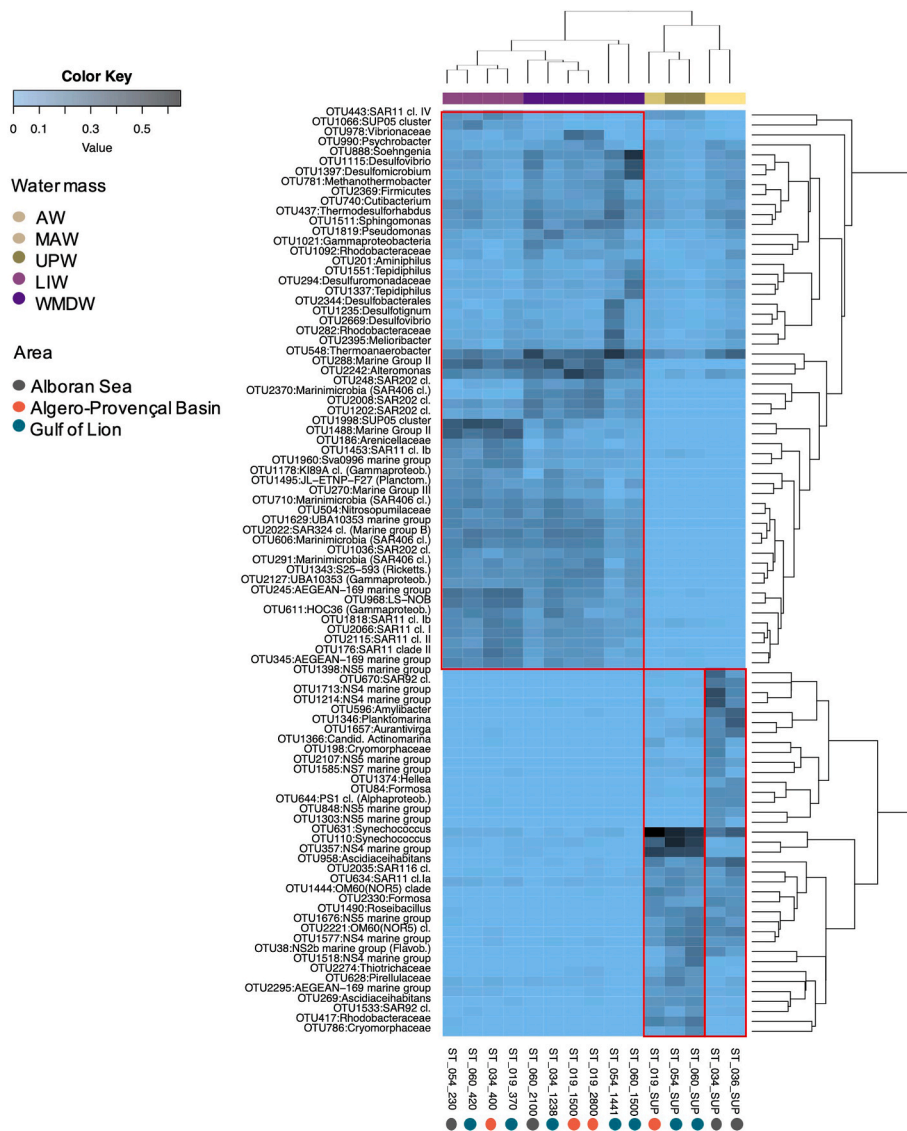
Fig. 4. Heatmap showing OTUs accounting for >1% as their maximum relative abundance in our dataset; red boxes show surface (AW and MAW + UPW) and deep (LIW and/or WMDW) diverse and exclusive sets of abundant OTUs; red boxes highlight the groups of differential, abundant taxa in surface and deep samples. "cl." = clade; "Flavob." = Flavobacteriaceae; "Gammaproteob." = Gammaprotebacteria; "Alphaproteob." = Alphaproteobacteria; "Planctom." = Planctomyceotota; "Ricketts." = Rickettsiaceae.

4.1. Surface waters

In surface waters, both quality of DOM (Table 1) and community composition differed between AW and MAW, suggesting that prokaryotes, being both consumers and producers of DOM, may change its optical properties. Notably, the AW was less enriched in Cyanobacteria and Planctomycetota, but more enriched in Firmicutes and Desulfobacterota compared to UPW and MAW. A peak of Flavobacteriales (Bacteroidota) was observed at ST34, together with the lowest surface a_{254}, $C1_{mh}$ and $C2_{th}$ and high $C3_p$ suggesting the presence of a fresh, less reworked DOM, that may have favoured the taxon that dominated at this station. This finding is in agreement with literature data showing that Flavobacteriaceae can typically grow when large amounts of dissolved proteins are available (Cottrell and Kirchman, 2000; Pinhassi et al., 2004).

The higher abundance of Cyanobacteria in the Gulf of Lion, mainly represented by *Synechococcus*, is coherent with the recent upwelling event, which brought to the surface nutrient-rich waters with DOM poor in proteins and rich in humic-like substances, thus likely favoring the growth of autotrophs. As to the nearly absence of *Prochlorococcus* in our samples, this was expected as it is known that *Prochlorococcus* prefers more oligotrophic conditions and generally dominates cyanobacterial populations at 50–60 m (Techtmann et al., 2015) up to 100–150 mt of

depth, which are depths not sampled in this study. In addition, Sebastián et al. (2021b) also confirmed the disappearance of *Prochlorococcus* in surface waters when moving from the Atlantic to the Mediterranean waters.

Across all surface stations, SAR11 was less abundant compared to data previously reported for surface seawater (avg., 40%; Agogué et al., 2011), also in the MS (up to an average of 37%, reviewed in Luna, 2015; between 9.5 and 35% as reported by Celussi et al., 2018). This result may also arise from the primer pair here used, which has been shown to underestimate the SAR11 clade (Wear et al., 2018). ST36 in the Alboran Sea showed a different community composition (i.e., higher relative abundance of other Alphaproteobacteria) when compared with ST34 in the same area and having similar hydrological properties. This station (ST36) exhibits indeed different DOM properties, such as lowest DOC and highest $S_{275-295}$ with respect to the other surface samples. The higher abundance of Alphaproteobacteria observed at this station, together with the highest surface $S_{275-295}$ (i.e. the lowest average molecular weight DOM), can be explained by the notion that Alphaproteobacteria are highly specialized in processing low molecular weight organic compounds (Alonso and Pernthaler, 2006; Del Giorgio and Gasol, 2008; Romera-Castillo et al., 2011). This observation provides further support to the existence of strong relationships between the DOM quality and microbial community composition. This is additionally
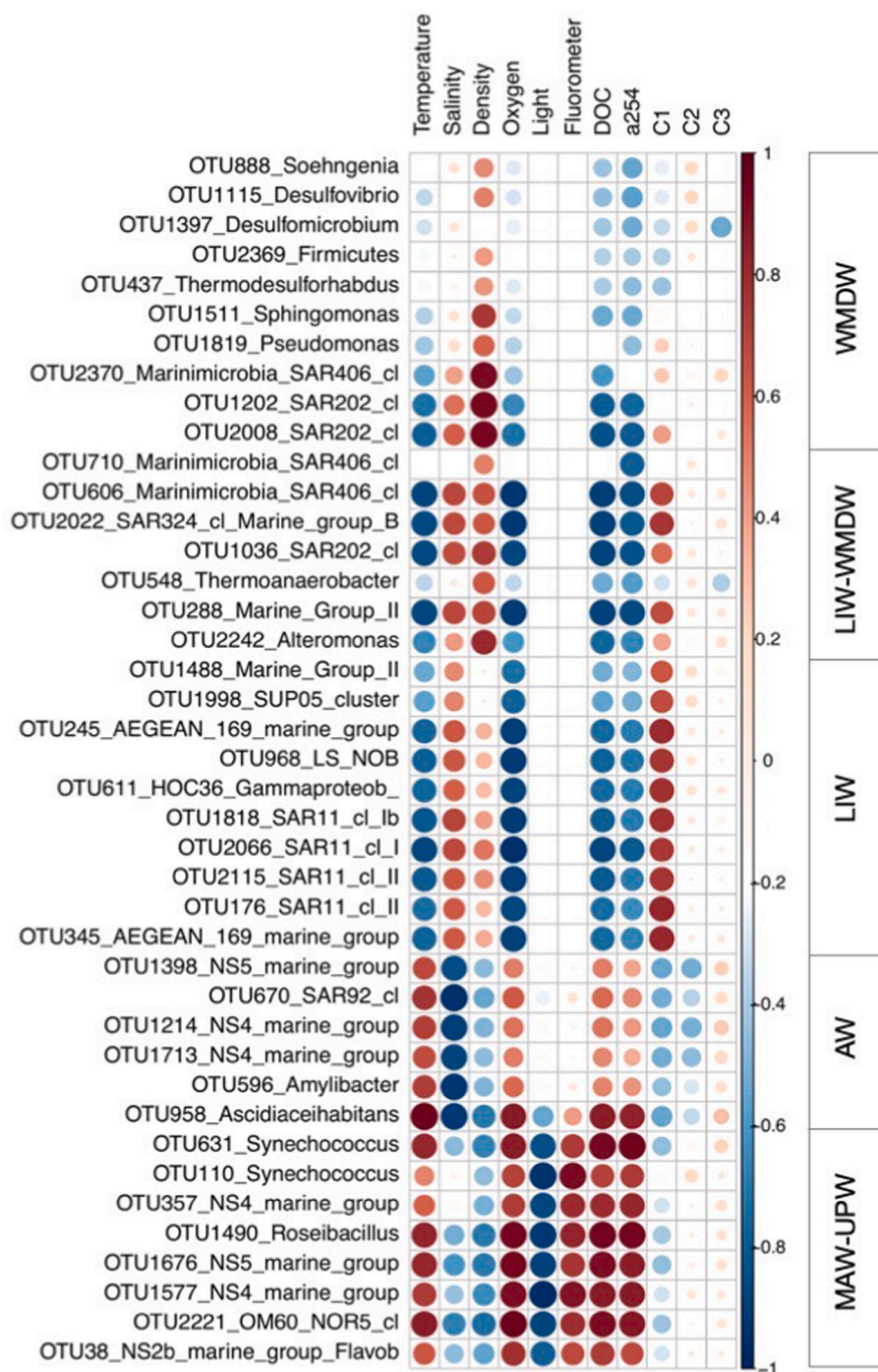
Fig. 5. Correlogram of the most abundant OTUs for the different water masses *vs.* environmental variables. Positive correlations are displayed in red and negative correlations in blue. Color intensity and the size of circles are proportional to the correlation coefficients. For LIW and WMDW, light and fluorometer were not included in this analysis. "cl" = clade; "Gammaproteob" = Gammaproteobacteria; "Flavob" = "Flavobacteriaceae".

corroborated by the significant positive relationships we have found between several surface taxa (eg, the Flavobacteriaceae members NS2b, NS4 and NS5 Marine Groups and the Rhodobacteraceae members *Amylibacter* and *Ascidiacehabitans*) and both DOC and a$_{254}$, which suggests the presence of a variety of metabolic strategies harbored by surface communities to exploit the different pools of DOM.

4.2. Levantine intermediate water (LIW)

At all the stations, the highest OTU richness was observed in the LIW. Particularly, the highest values were observed in correspondence with

the lowest oxygen concentration (highest AOU) and the highest C1$_{mh}$ fluorescence. This observation indicates that, with water mass ageing and therefore with the increase in recalcitrant DOM (evident by the high C1$_{mh}$ fluorescence), microbial community increases its diversity. The LIW is known to transport DOM that is progressively consumed by prokaryotes (Martínez–Pérez et al., 2019). Sebastián et al. (2021b) has recently hypothesized that Western MS mesopelagic waters hold more refractory DOM that selects for specific ASVs able to degrade it. Our findings support this hypothesis, as LIW waters, holding more re-fractory, low-molecular weight DOM, sustain more diverse microbial communities than surface and deep waters. In-depth analyses of our

samples show that such higher diversity in LIW samples was also sustained by a much higher contribution of rare members (<0.1% relative abundance) compared to surface and WMDW communities. The existence of these highly diversified microbial communities in dark layers, also including several rare taxa, may ensure their potential to quickly exploit sudden increases in fresh substrates associated to active transport by migrating animals (Steinberg et al., 2000; Calleja et al., 2018; Hernandez-Leon et al. 2019), sinking particles arriving to the deep layers (Smith et al., 2018) or dense water formation events (Tamburini et al., 2013; Luna et al., 2016; Severin et al., 2016). A similar association between recalcitrant DOM and high prokaryotic diversity has been also observed in the deep Labrador Sea (LaBrie et al., 2021) and has been associated with the presence of spatially constrained amplicon sequence variants that are capable to consume complex DOM molecules.

Interestingly, SAR11 consistently showed a peak in relative abundances in the LIW core at all stations, with particular reference to the clade II, which also include upper mesopelagic ecotypes (Giovannoni, 2017). Despite SAR11 clade is generally believed to show highest abundances in the ocean surface, recent studies similarly report the large contribution at comparable abundances in the LIW in the Western MS (Mena et al., 2021). In addition, several SAR11 ecotypes have been reported in the MS according to depth (Alonso-Sáez and Gasol, 2007; Rodríguez-Blanco et al., 2009; Luna et al., 2016; Giovannoni, 2017). It has been shown that seasonal blooms in SAR11 ecotype IIb may occur at intermediate depths during spring (Carlson et al., 2008, 2010), following a seasonal maximal DOC export from the surface and remineralization in the mesopelagic (Giovannoni, 2017). The increase in SAR11 with decreasing oxygen (i.e., with the ageing of the water) suggests that the observed peak in abundances of this clade in the LIW may be related to remineralization processes.

4.3. Western Mediterranean Deep Water

Abundant OTUs in the deep water masses (i.e., those shared between LIW and WMDW) displayed significant positive correlations with salinity and $C1_{mh}$, and negative correlations with temperature, oxygen, DOC and a_{254} (Fig. 5). Compared to LIW, prokaryotic communities in the deeper WMDW were overall dominated by Gammaproteobacteria, Desulfobacterota and Marinimicrobia (SAR406 clade), a result in accordance with numerous studies (Salazar et al., 2016; Celussi et al., 2018). Relatively high abundances of Planctomycetota and Chloroflexi, higher in the WMDW than in the LIW, were also observed in agreement with previous observations (Martín-Cuadrado et al., 2007; Celussi et al., 2018). Deep sea members of Chloroflexi (i.e., SAR202) have been previously shown to carry the gene for the 3-hydroxypropionate bi-cycle, and that they use this pathway for the assimilation of intermediate metabolisms produced by the degradation of recalcitrant DOM rather than for fixing CO_2 (Landry et al., 2017; Acinas et al., 2021), suggesting their key role in organic matter recycling in the deep sea. In the Gulf of Lion WMDW samples, a higher proportion of Desulfobacterota, Firmicutes and Actinobacteriota was observed. In these stations, the highest $S_{275-295}$ and $C2_{th}$, and the lowest $C1_{mh}$ and $C3_p$, were observed with respect of the other deep samples, suggesting that the occurrence of smaller and less aromatic DOM favors the growth of these taxa.

The archaeal relative contribution to prokaryotic assemblages increased with depth, confirming an established knowledge (Luna, 2015 and references therein; Celussi et al., 2018). The composition of archaeal assemblages in our study is in line with previous works in the Mediterranean, from the Ionian Sea (Zaballos et al., 2006) to the Thyrrenian (La Cono et al., 2009) and the Adriatic Sea (Luna et al., 2016). The relevance of Thermoplasmatota and Crenarchaeota (mainly Nitrosopumilaceae) differed in the LIW and the WMDW, with a higher relevance of Thermoplasmatota in the LIW than WMDW, a finding in contrast to the general pattern of Thaumarchaeota dominating over Thermoplasmatota (members of the former phylum Euryarchaeota) in the deep sea (Herndl et al., 2005; Teira et al., 2006; Salazar et al., 2016).

However, Thermoplasmatota members such as MGII (abundant in our deep samples) are often related to deep environments (in particular, groups B, C and D) (Massana et al., 2000; Martín-Cuadrado et al., 2007; Galand et al., 2009; Belmar et al., 2011; Hugoni et al., 2013; Quero et al., 2019) and have been already reported in the meso- and bathypelagic MS (Sebastián et al., 2021b). From a functional perspective, MGII has been proven to carry the genes for the production of large peptidases, and for a fatty acid degradation pathway, as well as a type II/IV secretion systems to transport proteins to the cell surface (Deschamps et al., 2014; Martin-Cuadrado et al., 2015); these findings suggest that protein degradation and utilization mechanisms are of particular importance for MGII metabolism, supporting the hypothesis of their heterotrophic lifestyle (Baker et al., 2013; Quero et al., 2019). MGII was indeed the most represented archaeal taxon in the dark Western MS, suggesting an important role played in the organic carbon processing in the deep MS (Boutrif et al., 2011), something that deserves to be examined further in future studies.

Most abundant OTUs in the deep Western MS included taxa previously described as abundant in the deep MS (the cosmopolitan deep-sea genus *Alteromonas* and SAR202) (Celussi et al., 2018) as well as at the global scale (*Alteromonas* and the gammaproteobacterial SUP05 cluster) (Dede et al., 2022; Salazar et al., 2016). The key ecological role of some of these taxa in the OM cycling in the deep ocean has been so far only partially clarified. Recent evidences indicate the ability of Alteromonadales to produce exopolysaccharides, which are further used to trap nutrients (Kumar et al., 2007; Gutierrez et al., 2013; Le Costaouëc et al., 2012). This finding suggests an increased efficiency in the processing of organic matter, even in a diluted environment (i.e. DOC 42–44 µM), by these deep sea heterotrophs. *Alteromonas* comprise copiotrophic taxa that display preference for a particle-associated lifestyle and have been suggested to have a cosmopolitan distribution throughout the water column using these particles as dispersion drivers (Mestre et al., 2017). In our study, *Alteromonas* was observed in both surface and deep layers, providing confirmation of its cosmopolitanism throughout the entire Western MS water column (as also previously reported by Sebastián et al., 2021a). Considering the preference of *Alteromonas* for nutrient-rich environments, its increased relative abundance in the deep waters suggests a determinant role played by this genus in the utilization of the DOC which is exported to deep MS layers.

5. Conclusions

We provide here evidence for a clear spatial structuring, as well a wide differentiation between depth, water masses and geographic areas, of pelagic prokaryotic communities throughout the water column in the Western MS. Also, we highlight, for the first time in the Western MS, significant links between DOM quantity and quality and microbial community structure, as already reported in other oceans such as the North Atlantic Ocean (Guerrero-Feijoo et al., 2017), providing evidence that communities are structured not only by the quantity, but also by the quality and composition of DOM. The coupling of spatially separated bacterial and archaeal communities (belonging to different water masses) with a different DOM quality, even at similar DOC concentrations, supports the idea that the different chemical properties can shape microbial communities, likely by creating different niches that support the growth of microbial taxa specialized in using DOM or in producing specific DOM compounds. More studies are certainly required to better elucidate the tight relationships between specific DOM-degrading prokaryotic taxa and their ability in processing DOM. Nonetheless, the data here provided may serve as basis for future studies on prokaryotic community structure in the MS basin, the environmental factors that drive this structure, and the potential of surface and deep sea prokaryotes to process labile and recalcitrant organic matter, in light of their role in the global carbon cycle and the changing conditions that are modifying the oceanography of the entire basin.

Author contributions

GML and CS designed the study. CS and SR collected the samples. GMQ and SR performed laboratory analyses. GMQ and GML performed bioinformatic and statistical analyses. GMQ, SR, CS and GML interpreted the data. GMQ and GML wrote the manuscript. All Authors provided the constructive comments, revised and edited the manuscript.

Declaration of competing interest

The authors declare that they have no known competing financial interests or personal relationships that could have appeared to influence the work reported in this paper.

Data availability

Sequence data are available at the NCBI SRA.

Acknowledgments

Appendix A. Supplementary data

Supplementary data to this article can be found online at https://doi.org/10.1016/j.dsr.2023.104022.

References

Acinas, S.G., Sánchez, P., Salazar, G., Cornejo-Castillo, F.M., Sebastián, M., Logares, R., et al., 2021. Deep ocean metagenomes provide insight into the metabolic architecture of bathypelagic microbial communities. Commun. Biol. 4, 604.

Agogué, H., Lamy, D., Neal, P.R., Sogin, M.L., Herndl, G.J., 2011. Water mass-specificity of bacterial communities in the North Atlantic revealed by massively parallel sequencing. Mol. Ecol. 20, 258–274.

Alonso, C., Pernthaler, J., 2006. *Roseobacter* and SAR11 dominate microbial glucose uptake in coastal North Sea waters. Environ. Microbiol. 8, 2022–2030.

Alonso-Sáez, L., Gasol, J.M., 2007. Seasonal variations in the contributions of different bacterial groups to the uptake of low-molecular-weight compounds in northwestern Mediterranean coastal waters. Appl. Environ. Microbiol. 73, 3528–3535.

Álvarez, M., Catalá, T.S., Civitarese, G., Coppola, L., Hassoun, A.E., Ibello, V., et al., 2023. Mediterranean Sea general biogeochemistry. In: Oceanography of the Mediterranean Sea. Elsevier, pp. 387–451.

Arístegui, J., Gasol, J.M., Duarte, C.M., Herndld, G.J., 2009. Microbial oceanography of the dark ocean's pelagic realm. Limnol. Oceanogr. 54, 1501–1529.

Baker, B.J., Sheik, C.S., Taylor, C.A., Jain, S., Bhasi, A., Cavalcoli, J.D., Dick, G.J., 2013. Community transcriptomic assembly reveals microbes that contribute to deep-sea carbon and nitrogen cycling. ISME J. 7, 1962–1973.

Belmar, L., Molina, V., Ulloa, O., 2011. Abundance and phylogenetic identity of archaeoplankton in the permanent oxygen minimum zone of the eastern tropical South Pacific. FEMS Microb. Ecol. 78, 314–326.

Boutrif, M., Garel, M., Cottrell, M.T., Tamburini, C., 2011. Assimilation of marine extracellular polymeric substances by deep-sea prokaryotes in the NW Mediterranean Sea. Environ. Microbiol. Rep. 3, 705–709.

Burd, A.B., Hansell, D.A., Steinberg, D.K., Anderson, T.R., Arístegui, J., Baltar, F., et al., 2010. Assessing the apparent imbalance between geochemical and biochemical indicators of meso- and bathypelagic biological activity: what the @$#! is wrong with present calculations of carbon budgets? Deep Sea Res. II 57, 1557–1571.

Calleja, M.L., Ansari, M.I., Røstad, A., Silva, L., Kaartvedt, S., Irigoien, X., Morán, X.A.G., 2018. The mesopelagic scattering layer: a hotspot for heterotrophic prokaryotes in the Red Sea twilight zone. Front. Mar. Sci. 5, 259.

Caporaso, J.G., Kuczynski, J., Stombaugh, J., Bittinger, K., Bushman, F.D., Costello, E.K., et al., 2010. QIIME allows analysis of high-throughput community sequencing data. Nat. Methods 7, 335–336.

Carlson, C.A., Hansell, D.A., Nelson, N.B., Siegel, D.A., Smethie, W.M., Khatiwala, S., et al., 2010. Dissolved organic carbon export and subsequent remineralization in the mesopelagic and bathypelagic realms of the North Atlantic basin. Deep-Sea Res. Part II 57, 1433–1445.

Carlson, C.A., Morris, R., Parsons, R., Treusch, A.H., Giovannoni, S.J., Vergin, K., 2008. Seasonal dynamics of SAR11 populations in the euphotic and mesopelagic zones of the northwestern Sargasso Sea. ISME J. 3, 283–295.

Celussi, M., Quero, G.M., Zoccarato, L., Franzo, A., Corinaldesi, C., Rastelli, E., et al., 2018. Planktonic prokaryote and protist communities in a submarine canyon system in the Ligurian Sea (NW Mediterranean). Prog. Oceanogr. 168, 210–221.

Coll, M., Piroddi, C., Steenbeek, J., Kaschner, K., Lasram, F.B.R., Aguzzi, J., et al., 2010. The biodiversity of the Mediterranean Sea: estimates, patterns, and threats. PLoS One 5, e11842.

Cottrell, M.T., Kirchman, D.L., 2000. Natural assemblages of marine proteobacteria and members of the Cytophaga-Flavobacter cluster consuming low-and high-molecular-weight dissolved organic matter. Appl. Environ. Microbiol. 66, 1692–1697.

De Corte, D., Yokokawa, T., Varela, M.M., Agogue, H., Herndl, G.J., 2009. Spatial distribution of bacteria and archaea and amoA gene copy numbers throughout the water column of the eastern Mediterranean Sea. ISME J. 3, 147–158.

Dede, B., Hansen, C.T., Neuholz, R., Schnetger, B., Kleint, C., Walker, S., et al., 2022. Niche differentiation of sulfur-oxidizing bacteria (SUP05) in submarine hydrothermal plumes. ISME J. 16, 1479–1490.

Del Giorgio, P.A., Gasol, J.M., 2008. Physiological structure and single cell activity in marine bacterioplankton, p. 243–285. In: Kirchman, D.L. (Ed.), Microbial Ecology of the Oceans, second ed. Wiley-Blackwell, Hoboken, NJ.

Del Vecchio, R., Blough, N.V., 2004. Spatial and seasonal distribution of chromophoric dissolved organic matter and dissolved organic carbon in the Middle Atlantic Bight. Mar. Chem. 89, 169–187.

Deschamps, P., Zivanovic, Y., Moreira, D., Rodriguez-Valera, F., López-García, P., 2014. Pangenome evidence for extensive interdomain horizontal transfer affecting lineage core and shell genes in uncultured planktonic thaumarchaeota and euryarchaeota. Genome Biology and Evolution 6, 1549–1563.

Dittmar, T., Lennartz, S.T., Buck-Wiese, H., Hansell, D.A., Santinelli, C., Vanni, C., et al., 2021. Enigmatic persistence of dissolved organic matter in the ocean. Nat. Rev. Earth Environ. 2, 570–583.

Dobal-Amador, V., Nieto-Cid, M., Guerrero-Feijoo, E., Hernando-Morales, V., Teira, E., Varela, M.M., 2016. Vertical stratification of bacterial communities driven by multiple environmental factors in the waters (0–5000 m) off the Galician coast (NW Iberian margin). Deep Sea Res. Oceanogr. Res. Pap. 114, 1–11.

Edgar, R.C., 2010. Search and clustering orders of magnitude faster than BLAST. Bioinformatics 26, 2460–2461.

Eiler, A., Heinrich, F., Bertilsson, S., 2012. Coherent dynamics and association networks among lake bacterioplankton taxa. ISME J. 6, 330–342.

Galand, P.E., Casamayor, E.O., Kirchman, D.L., Potvin, M., Lovejoy, C., 2009. Unique archaeal assemblages in the Arctic Ocean unveiled by massively parallel tag sequencing. ISME J. 3, 860–869.

Galletti, Y., Gonnelli, M., Brogi, S.R., Vestri, S., Santinelli, C., 2019. DOM dynamics in open waters of the Mediterranean Sea: new insights from optical properties. Deep Sea Res. Oceanogr. Res. Pap. 144, 95–114.

Giorgi, F., 2006. Climate change hot-spots. Geophys. Res. Lett. 33, L08707.

Giovannoni, S.J., 2017. SAR11 bacteria: the most abundant plankton in the oceans. Ann. Rev. Mar. Sci 9, 231–255.

Giuliano, L., De Domenico, M., De Domenico, E., Höfle, M.G., Yakimov, M.M., 1999. Identification of culturable oligotrophic bacteria within naturally occurring bacterioplankton communities of the Ligurian Sea by 16S rRNA sequencing and probing. Microb. Ecol. 37, 77–85.

Gu, Z., 2016. Complex heatmaps reveal patterns and correlations in multidimensional genomic data. Bioinformatics 32, 2847–2849.

Guerrero-Feijoo, E., Nieto-Cid, M., Sintes, E., Dobal-Amador, V., Hernando-Morales, V., Alvarez, M., et al., 2017. Optical properties of dissolved organic matter relate to different depth-specific patterns of archaeal and bacterial community structure in the North Atlantic Ocean. FEMS Microbiol. Ecol. 93, fiw224.

Gutierrez, T., Berry, D., Yang, T., Mishamandani, S., McKay, L., Teske, A., Aitken, M.D., 2013. Role of bacterial exopolysaccharides (eps) in the fate of the oil released during the deepwater horizon oil spill. PLoS One 8, e67717.

Hansell, D.A., 2005. Dissolved Organic Carbon Reference Material Program, 86. Eos Transaction American Geophysics Union, p. 318.

Hansell, D.A., 2013. Recalcitrant dissolved organic carbon fractions. Ann. Rev. Mar. Sci 5, 421–445.

Helms, J.R., Stubbins, A., Ritchie, J.D., Minor, E.C., Kieber, D.J., Mopper, K., 2008. Absorption spectral slopes and slope ratios as indicators of molecular weight, source, and photobleaching of chromophoric dissolved organic matter. Limnol. Oceanogr. 53, 955–969.

Herndl, G.J., Reinthaler, T., Teira, E., van Aken, H., Veth, C., Pernthaler, A., Pernthaler, J., 2005. Contribution of Archaea to total prokaryotic production in the deep Atlantic Ocean. Appl. Environ. Microbiol 71, 2303–2309.

Hugoni, M., Taib, N., Debroas, D., Domaizon, I., Jouan Dufournel, I., Bronner, G., et al., 2013. Structure of the rare archaeal biosphere and seasonal dynamics of active ecotypes in surface coastal waters. Proc. Natl. Acad. Sci. U.S.A. 110, 6004–6009.

Kindt, R., Coe, R., 2005. Tree Diversity Analysis. A Manual and Software for Common Statistical Methods for Ecological and Biodiversity Studies. World Agroforestry Centre (ICRAF), Nairobi (Kenya), ISBN 92-9059-179-X. http://www.worldagroforestry.org/output/tree-diversity-analysis.

Korlević, M., Ristova, P.P., Garić, R., Amann, R., Orlić, S., 2015. Bacterial diversity in the South Adriatic Sea during a strong, deep winter convection year. Appl. Environ. Microbiol. 81, 1715–1726.

Kumar, A.S., Mody, K., Jha, B., 2007. Bacterial exopolysaccharides—a perception. J. Basic Microbiol. 47, 103–117.

La Cono, V., Tamburini, C., Genovese, L., La Spada, G., Denaro, R., Yakimov, M.M., 2009. Cultivation-independent assessment of the bathypelagic archaeal diversity of Tyrrhenian Sea: Comparative study of rDNA and rRNA-derived libraries and influence of sample decompression. Deep Sea Res. Part II Top. Stud. Oceanogr. 56, 768–773.

LaBrie, R., Bélanger, S., Benner, R., Maranger, R., 2021. Spatial abundance distribution of prokaryotes is associated with dissolved organic matter composition and ecosystem function. Limnol. Oceanogr. 66, 575–587.

Landry, Z., Swan, B.K., Herndl, G.J., Stepanauskas, R., Giovannoni, S.J., 2017. SAR202 genomes from the dark ocean predict pathways for the oxidation of recalcitrant dissolved organic matter. MBio 8, e00413–17.

Le Costaouëc, T., Cérantola, S., Ropartz, D., Ratiskol, J., Sinquin, C., Colliec-Jouault, S., Boisset, C., 2012. Structural data on a bacterial exopolysaccharide produced by a deep-sea Alteromonas macleodii strain. Carbohydr. Polym. 90, 49–59.

López-López, A., Bartual, S.G., Stal, L., Onyshchenko, O., Rodríguez-Valera, F., 2005. Genetic analysis of housekeeping genes reveals a deep-sea ecotype of Alteromonas macleodii in the Mediterranean Sea. Environ. Microbiol. 7, 649–659.

Luna, G.M., 2015. Diversity of marine microbes in a changing Mediterranean Sea. Rendiconti Lincei 26, 49–58.

Luna, G.M., Bianchelli, S., Decembrini, F., De Domenico, E., Danovaro, R., Dell'Anno, A., 2012. The dark portion of the Mediterranean Sea is a bioreactor of organic matter cycling. Global Biogeochem. Cycles 26 (2).

Luna, G.M., Chiggiato, J., Quero, G.M., Schroeder, K., Bongiorni, L., Kalenitchenko, D., Galand, P.E., 2016. Dense water plumes modulate richness and productivity of deep sea microbes. Environ. Microbiol. 18, 4537–4548.

Mapelli, F., Varela, M.M., Barbato, M., Alvarino, R., Fusi, M., Álvarez, M., et al., 2013. Biogeography of planktonic microbial communities across the whole Mediterranean Sea. Ocean Sci. Discuss. 10, 585–595.

Martin-Cuadrado, A.B., Garcia-Heredia, I., Molto, A.G., Lopez-Ubeda, R., Kimes, N., López-García, P., et al., 2015. A new class of marine Euryarchaeota group II from the mediterranean deep chlorophyll maximum. ISME J 9, 1619–1634.

Martín-Cuadrado, A.B., López-García, P., Alba, J.C., Moreira, D., Monticelli, L., Strittmatter, A., et al., 2007. Metagenomics of the deep Mediterranean, a warm bathypelagic habitat. PLoS One 2, e914.

Martínez–Pérez, A.M., Catalá, T.S., Nieto–Cid, M., Otero, J., Álvarez, M., Emelianov, M., et al., 2019. Dissolved organic matter (DOM) in the open Mediterranean Sea. II: basin–wide distribution and drivers of fluorescent DOM. Prog. Oceanogr. 170, 93–106.

Massana, R., DeLong, E.F., Pedrós-Alió, C., 2000. A few cosmopolitan phylotypes dominate planktonic archaeal assemblages in widely different oceanic provinces. Appl. Environ. Microbiol. 66, 1777–1787.

Mena, C., Balbín, R., Reglero, P., Martín, M., Santiago, R., Sintes, E., 2021. Dynamic prokaryotic communities in the dark western Mediterranean Sea. Sci. Rep. 11, 1–14.

Mende, D.R., Bryant, J.A., Aylward, F.O., Eppley, J.M., Nielsen, T., Karl, D.M., DeLong, E.F., 2017. Environmental drivers of a microbial genomic transition zone in the ocean's interior. Nat. Microbiol. 2, 1367–1373.

Mestre, M., Ferrera, I., Borrull, E., Ortega-Retuerta, E., Mbedi, S., Grossart, H.P., et al., 2017. Spatial variability of marine bacterial and archaeal communities along the particulate matter continuum. Mol. Ecol. 26 (24), 6827–6840.

Murphy, K.R., Stedmon, C.A., Graeber, D., Bro, R., 2013. Fluorescence spectroscopy and multi-way techniques. PARAFAC. Anal. Methods 5, 6557–6566.

Murphy, K.R., Stedmon, C.A., Wenig, P., Bro, R., 2014. OpenFluor–an online spectral library of auto-fluorescence by organic compounds in the environment. Anal. Methods 6, 658–661.

Omanović, D., Santinelli, C., Marcinek, S., Gonnelli, M., 2019. ASFit-An all-inclusive tool for analysis of UV–Vis spectra of colored dissolved organic matter (CDOM). Comput. Geosci. 133, 104334.

Pinhassi, J., Sala, M.M., Havskum, H., Peters, F., Guadayol, O., Malits, A., Marrasé, C., 2004. Changes in bacterioplankton composition under different phytoplankton regimens. Appl. Environ. Microbiol. 70, 6753–6766.

Quero, G.M., Celussi, M., Relitti, F., Kovačević, V., Del Negro, P., Luna, G.M., 2019. Inorganic and organic carbon uptake processes and their connection to microbial diversity in meso-and bathypelagic arctic waters (eastern fram strait). Microb. Ecol. 79, 1–17.

Quero, G.M., Perini, L., Pesole, G., Manzari, C., Lionetti, C., Bastianini, M., et al., 2017. Seasonal rather than spatial variability drives planktonic and benthic bacterial diversity in a microtidal lagoon and the adjacent open sea. Mol. Ecol. 26, 5961–5973.

Rahav, E., Silverman, J., Raveh, O., Hazan, O., Rubin-Blum, M., Zeri, C., et al., 2019. The deep water of Eastern Mediterranean Sea is a hotspot for bacterial activity. Deep Sea Res. Part II Top. Stud. Oceanogr. 164, 135–143.

Retelletti Brogi, S., Gonnelli, M., Vestri, S., Santinelli, C., 2015. Biophysical processes affecting DOM dynamics at the Arno river mouth (Tyrrhenian Sea). Biophys. Chem. 197, 1–9.

Rodríguez-Blanco, A., Ghiglione, J.F., Catala, P., Casamayor, E.O., Lebaron, P., 2009. Spatial comparison of total vs. active bacterial populations by coupling genetic fingerprinting and clone library analyses in the NW Mediterranean Sea. FEMS Microbiol. Ecol. 67, 30–42.

Romera-Castillo, C., Sarmento, H., Alvarez-Salgado, X.A., Gasol, J.M., Marrasé, C., 2011. Net production and consumption of fluorescent colored dissolved organic matter by natural bacterial assemblages growing on marine phytoplankton exudates. Appl. Environ. Microbiol. 77, 7490–7498.

RStudio Team, 2015. RStudio. Integrated Development for R. RStudio, Inc., Boston, MA. URL. http://www.rstudio.com/.

Salazar, G., Cornejo-Castillo, F.M., Benítez-Barrios, V., Fraile-Nuez, E., Álvarez-Salgado, X.A., Duarte, C.M., et al., 2016. Global diversity and biogeography of deep-sea pelagic prokaryotes. ISME J. 10, 596–608.

Santinelli, C., 2015. DOC in the Mediterranean Sea. In: Biogeochemistry of Marine Dissolved Organic Matter. Academic Press, pp. 579–608.

Santinelli, C., Follett, C., Retelletti Brogi, S., Xu, L., Repeta, D., 2015. Carbon isotope measurements reveal unexpected cycling of dissolved organic matter in the deep Mediterranean Sea. Mar. Chem. 177, 267–277.

Santinelli, C., Nannicini, L., Seritti, A., 2010. DOC dynamics in the meso and bathypelagic layers of the Mediterranean Sea. Deep Sea Res. Part II Top. Stud. Oceanogr. 57, 1446–1459.

Schroeder, K., Chiggiato, J., Bryden, H.L., Borghini, M., Ismail, S.B., 2016. Abrupt climate shift in the western Mediterranean Sea. Sci. Rep. 6, 23009.

Sebastián, M., Forn, I., Auladell, A., Gómez-Letona, M., Sala, M.M., Gasol, J.M., Marrasé, C., 2021a. Differential recruitment of opportunistic taxa leads to contrasting abilities in carbon processing by bathypelagic and surface microbial communities. Environ. Microbiol. 23, 190–206.

Sebastián, M., Ortega-Retuerta, E., Gómez-Consarnau, L., Zamanillo, M., Álvarez, M., Arístegui, J., Gasol, J.M., 2021b. Environmental gradients and physical barriers drive the basin-wide spatial structuring of Mediterranean Sea and adjacent eastern Atlantic Ocean prokaryotic communities. Limnol. Oceanogr. 66, 4077–4095.

Severin, T., Sauret, C., Boutrif, M., Duhaut, T., Kessouri, F., Oriol, L., et al., 2016. Impact of an intense water column mixing (0–1500 m) on prokaryotic diversity and activities during an open-ocean convection event in the NW Mediterranean Sea. Environ. Microbiol. 18, 4378–4390.

Siokou-Frangou, I., Christaki, U., Mazzocchi, M.G., Montresor, M., Ribera d'Alcalà, M., Vaqué, D., Zingone, A., 2010. Plankton in the open Mediterranean Sea: a review. Biogeosciences 7, 1543–1586.

Tamburini, C., Garel, M., Al Ali, B., Mérigot, B., Kriwy, P., Charrière, B., et al., 2009. Distribution and activity of bacteria and archaea in the different water masses of the Tyrrhenian Sea. Deep Sea Res. Part II Top. Stud. Oceanogr. 56, 700–712.

Smith Jr., K.L., Ruhl, H.A., Huffard, C.L., Messié, M., Kahru, M., 2018. Episodic organic carbon fluxes from surface ocean to abyssal depths during long-term monitoring in NE Pacific. Proc. Natl. Acad. Sci. U.S.A. 115, 12235–12240.

Steinberg, D.K., Carlson, C.A., Bates, N.R., Goldthwait, S.A., Madin, L.P., Michaels, A.F., 2000. Zooplankton vertical migration and the active transport of dissolved organic and inorganic carbon in the Sargasso Sea. Deep Sea Res. Part I Oceanogr. Res. Pap. 47, 137–158.

Tamburini, C., Boutrif, M., Garel, M., Colwell, R.R., Deming, J.W., 2013. Prokaryotic responses to hydrostatic pressure in the ocean–a review. Environ. Microbiol. 15, 1262–1274.

Techtmann, S.M., Fortney, J.L., Ayers, K.A., Joyner, D.C., Linley, T.D., Pfiffner, S.M., Hazen, T.C., 2015. The unique chemistry of Eastern Mediterranean water masses selects for distinct microbial communities by depth. PLoS One 10, e0120605.

Teira, E., Lebaron, P., Van Aken, H., Herndl, G.J., 2006. Distribution and activity of Bacteria and Archaea in the deep water masses of the North Atlantic. Limnol. Oceanogr. 51, 2131–2144.

Wear, E.K., Wilbanks, E.G., Nelson, C.E., Carlson, C.A., 2018. Primer selection impacts specific population abundances but not community dynamics in a monthly time-series 16S rRNA gene amplicon analysis of coastal marine bacterioplankton. Environ. Microbiol. 20, 2709–2726.

Wei, T, Simko, V. R package 'corrplot': Visualization of a Correlation Matrix. (Version 0.92). https://github.com/taiyun/corrplot.

Zaballos, M., Lopez-Lopez, A., Ovreas, L., Bartual, S.G., D'Auria, G., Alba, J.C., et al., 2006. Comparison of prokaryotic diversity at offshore oceanic locations reveals a different microbiota in the Mediterranean Sea. FEMS Microbiol. Ecol. 56, 389–405.

Supplementary Material

Water mass age and dissolved organic matter properties drive the diversity of pelagic prokaryotes in the Western Mediterranean Sea

Grazia Marina Quero[1,2*], Simona Retelletti Brogi[3,4], Chiara Santinelli[2,3], Luna Gian Marco[1,2]

[1]Institute for Biological Resources and Marine Biotechnologies, National Research Council (IRBIM-CNR), Largo Fiera della Pesca 2, 60125, Ancona, Italy

[2] National Biodiversity Future Center (NBFC), 90133 Palermo, Italy

[3] Biophysics Institute, National Research Council (IBF-CNR), Via G. Moruzzi, Pisa 56124, Italy

[4]Istituto di Oceanografia e Geofisica Sperimentale (OGS) - Sezione di Oceanografia, Borgo Grotta Gigante 42/C, Sgonico (TS) 34010, Italia

* Correspondence:

grazia.quero@irbim.cnr.it

Supplementary Tables 1 and 2

Supplementary Figures 1, 2, 3, 4, 5, 6, 7, 8

Supplementary References

Table S1. Details of the sampling stations.

Area	Station	Sampling date	Sampling Time	Lat °N	Lon °E	Bottom Depth (m)
Algero-Provençal Basin	19	14/04/14	22:07	38.5013	2.5478	2700
Alboran Sea	34	17/04/14	08:58	36.0498	-3.8496	1250
	36	18/04/14	10:00	36.1413	-4.4405	1163
Gulf of Lion	54	22/04/14	20:11	41.568	3.6626	1450
	60	23/04/14	19:50	42.253	4.696	2120
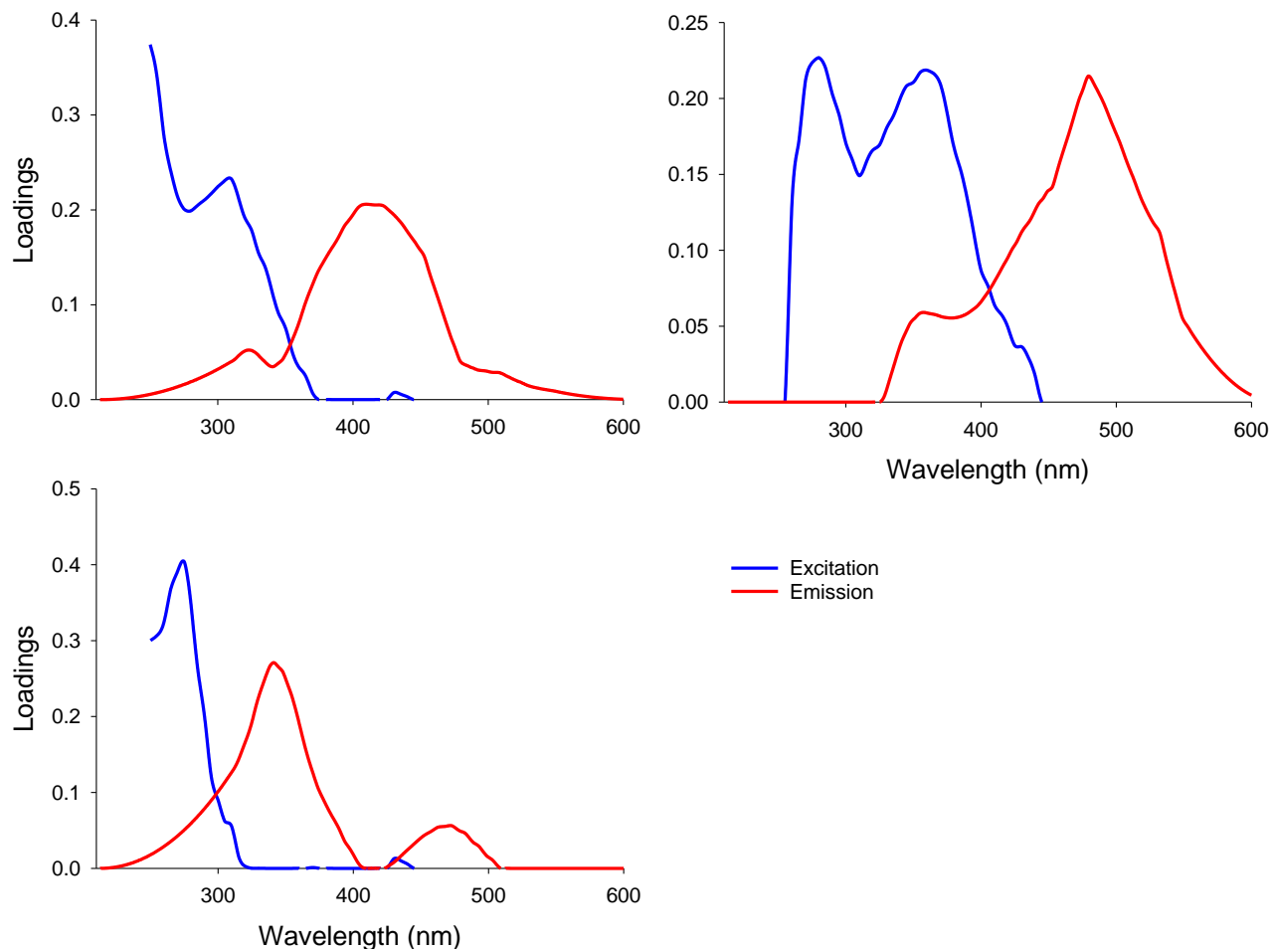
Figure S1. Excitation (blue) and emission (red) spectra of the three components validated by the PARAFAC analysis.

Table S2. Excitation and emission maxima of the components validated by PARAFAC analysis, their identification and comparison with similar components reported in the literature.

Component	λex max (nm)	λem max (nm)	Identification	Similar components
C1	<250, 310	409	Microbial humic-like	Cawley et al., 2012 Gao & Gueguen, 2017 Yamashita et al., 2021 Chen et al., 2018
C2	280 - 360	479	Terrestrial Humic-like	Li et al., 2015 Dainard et al., 2015 Català et al., 2015 Yamashita et al., 2010
C3	275	341	Protein-like	Wünsch et al., 2017 Lapierre & Del Giorgio 2014 Krylov et al., 2020 Bittar et al., 2015

References
Catalá et al. 2015. Turnover time of fluorescent dissolved organic matter in the dark global ocean. Nat. Commun. 6: 5986.
Cawley et al. 2012. Characterizing the sources and fate of dissolved organic matter in Shark Bay, Australia: a preliminary study using optical properties and stable carbon isotopes. Marine and Freshwater Research, v63, p1098-1107.
Chen et al. 2018. Surface accumulation of low molecular weight dissolved organic matter in surface waters and horizontal off-shelf spreading of nutrients and humic-like fluorescence in the Chukchi Sea of the Arctic Ocean, Science of the Total Environment, 639, 624-632.
Dainard et al. 2015. Photobleaching of fluorescent dissolved organic matter in Beaufort Sea and North Atlantic Subtropical Gyre, Mar. Chem., 177, 630-637.
Gao and Gueguen 2017. Size distribution of absorbing and fluorescing DOM in Beaufort Sea, Canada Basin. Deep-Sea Research Part I, 121, 30-37.
Krylov et al., 2020. Albatross R package to study PARAFAC components of DOM fluorescence from mixing zones of arctic shelf seas, Chemometrics and Intelligent Laboratory Systems. 207, 104176.
Lapierre and del Giorgio 2014. Partial coupling and differential regulation of biologically and photochemically labile dissolved organic carbon across boreal aquatic networks. Biogeosciences 11, 5969–5985.
Li et al. 2015. Spatiotemporal Distribution, Sources, and Photobleaching Imprint of Dissolved Organic Matter in the Yangtze Estuary and Its Adjacent Sea Using Fluorescence and Parallel Factor Analysis. PLoS ONE 10(6): e0130852.
Wünsch et al. 2017. The one-sample PARAFAC approach reveals molecular size distributions of fluorescent components in dissolved organic matter, Environmental Science & Technology, 51 (20)
Yamashita et al. 2010. Fluorescence characteristics of dissolved organic matter in the deep waters of the Okhotsk Sea and the northwestern North Pacific Ocean. Deep-Sea Res II 57, 1478-1485.
Yamashita et al. 2021. Relationships between dissolved black carbon and dissolved organic matter in streams, Chemosphere, 271, 129824.
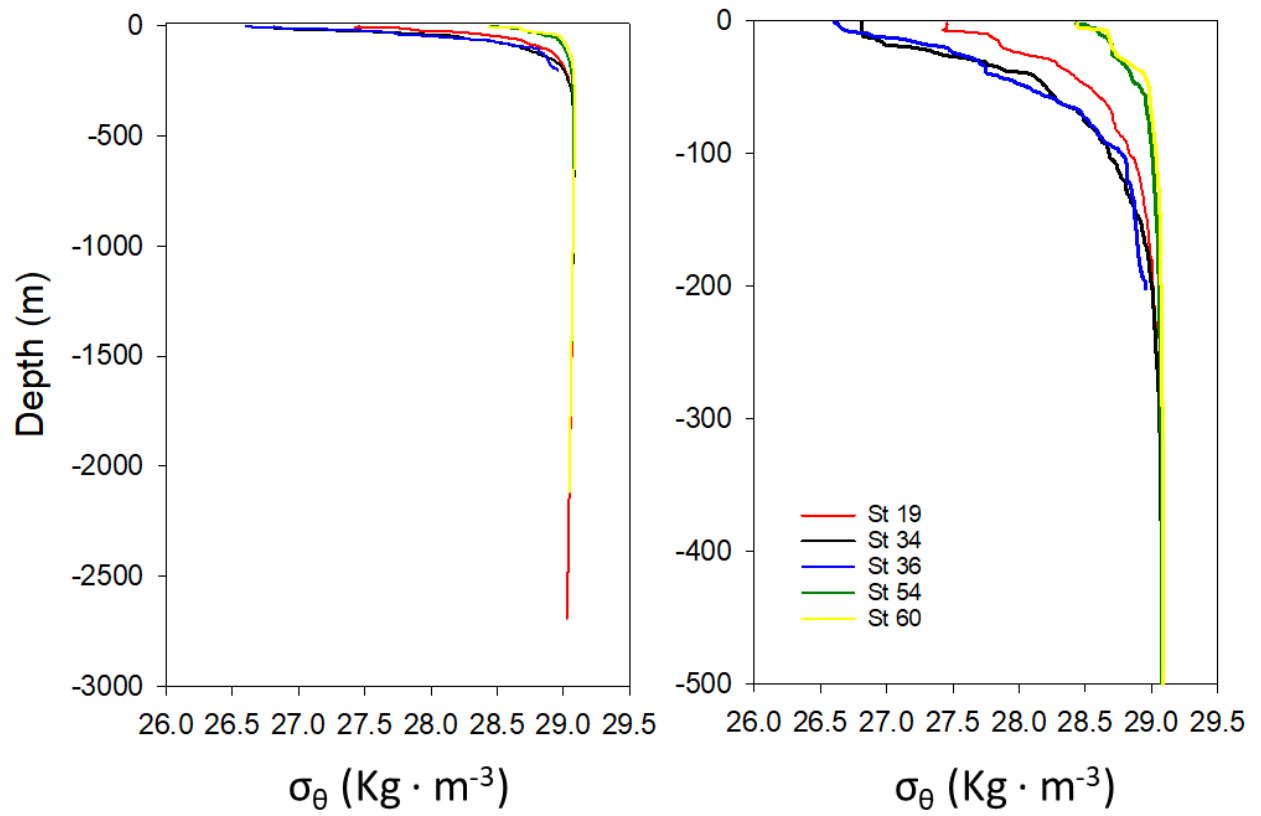
Figure S2. Vertical profiles of density of the sampled stations (left), with a zoom of the upper 500 m (right).
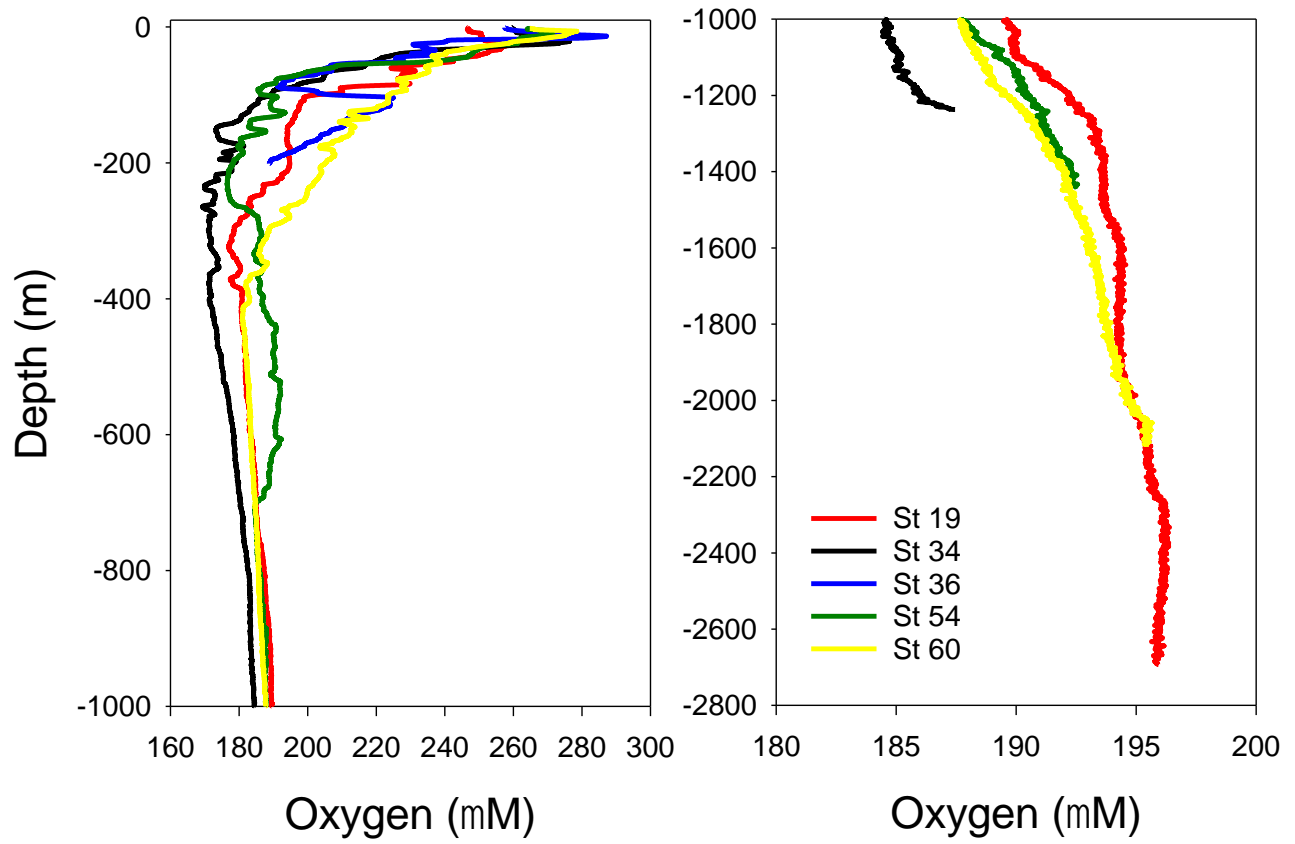
Figure S3. Vertical profiles of dissolved oxygen of the sampled stations in the first 1000m (left), and from 1000 m to the bottom (right).
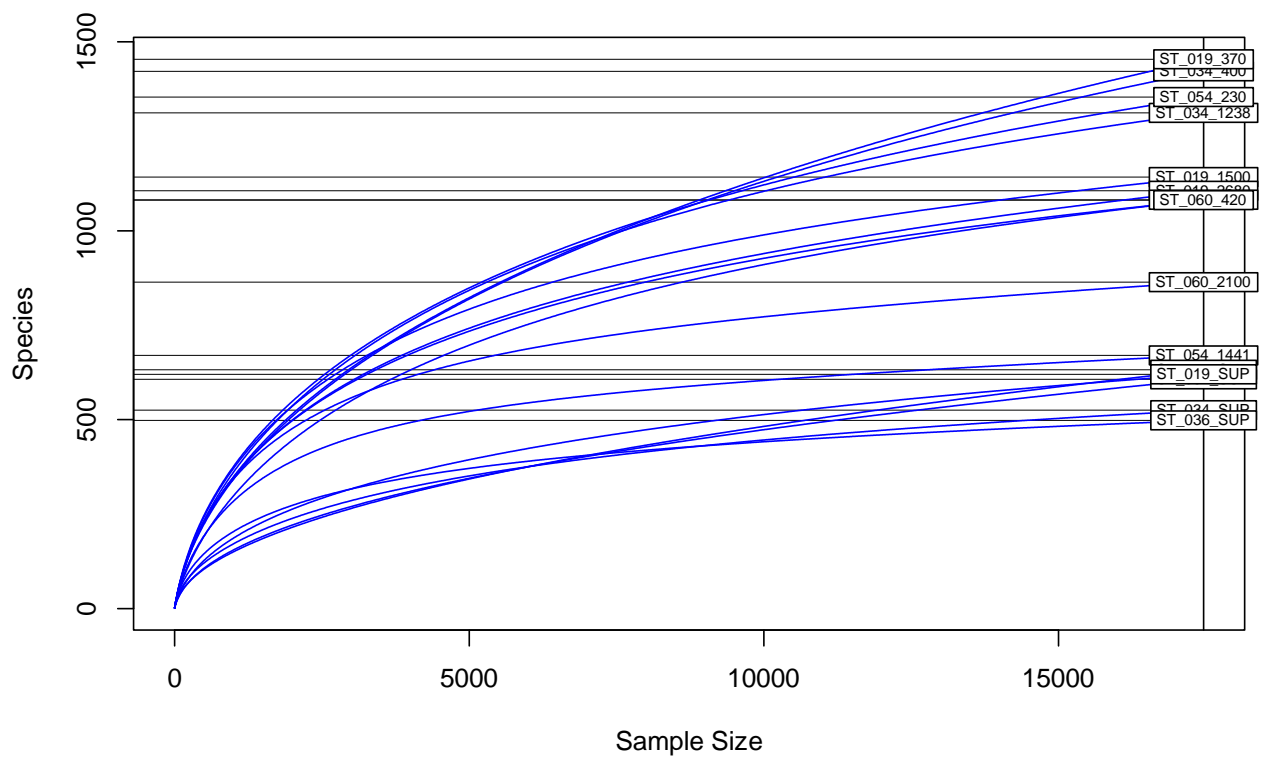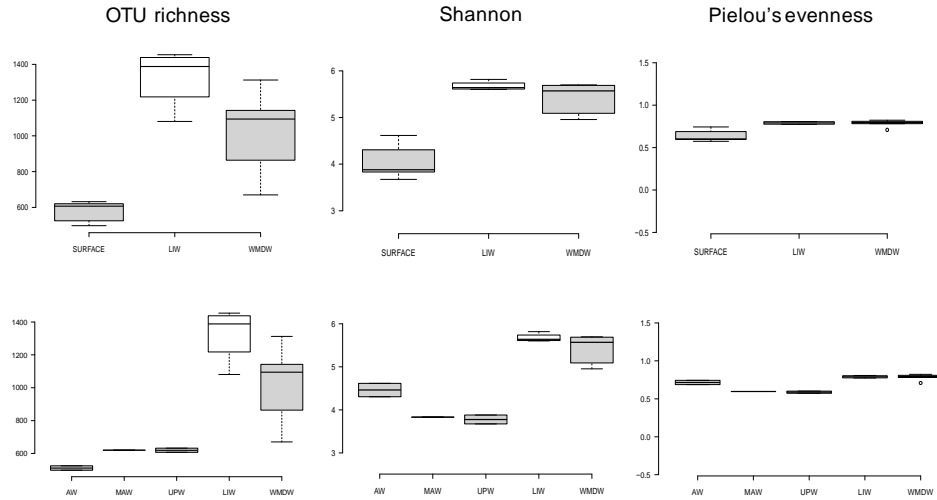
Figure S4. Rarefaction curves showing the number of OTUs (97%; "species") compared to the number of reads (sample size) observed in the total dataset.
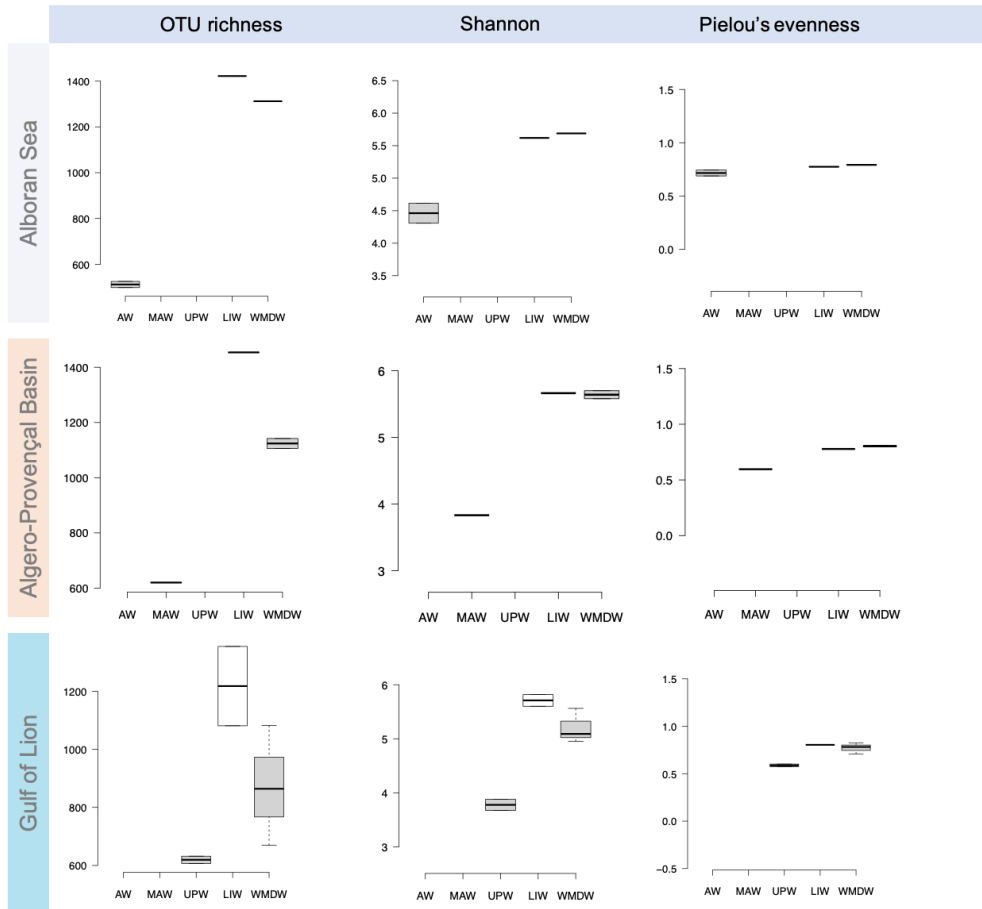
Figure S5. Alpha diversity. Panel A shows values for OTU richness, Pielou's evenness and Shannon index for samples grouped by depth; upper and lower plots show surface samples grouped together (upper) or separated by mass (lower). Panel B show, per each studied area and depth, OTU richness, Shannon index and Pielou's evenness, respectively. AW: Atlantic Water; MAW: Modified Atlantic Water; UPW: upwelling waters; LIW: Levantine Intermediate Water; WMDW: West Mediterranean Deep Water.
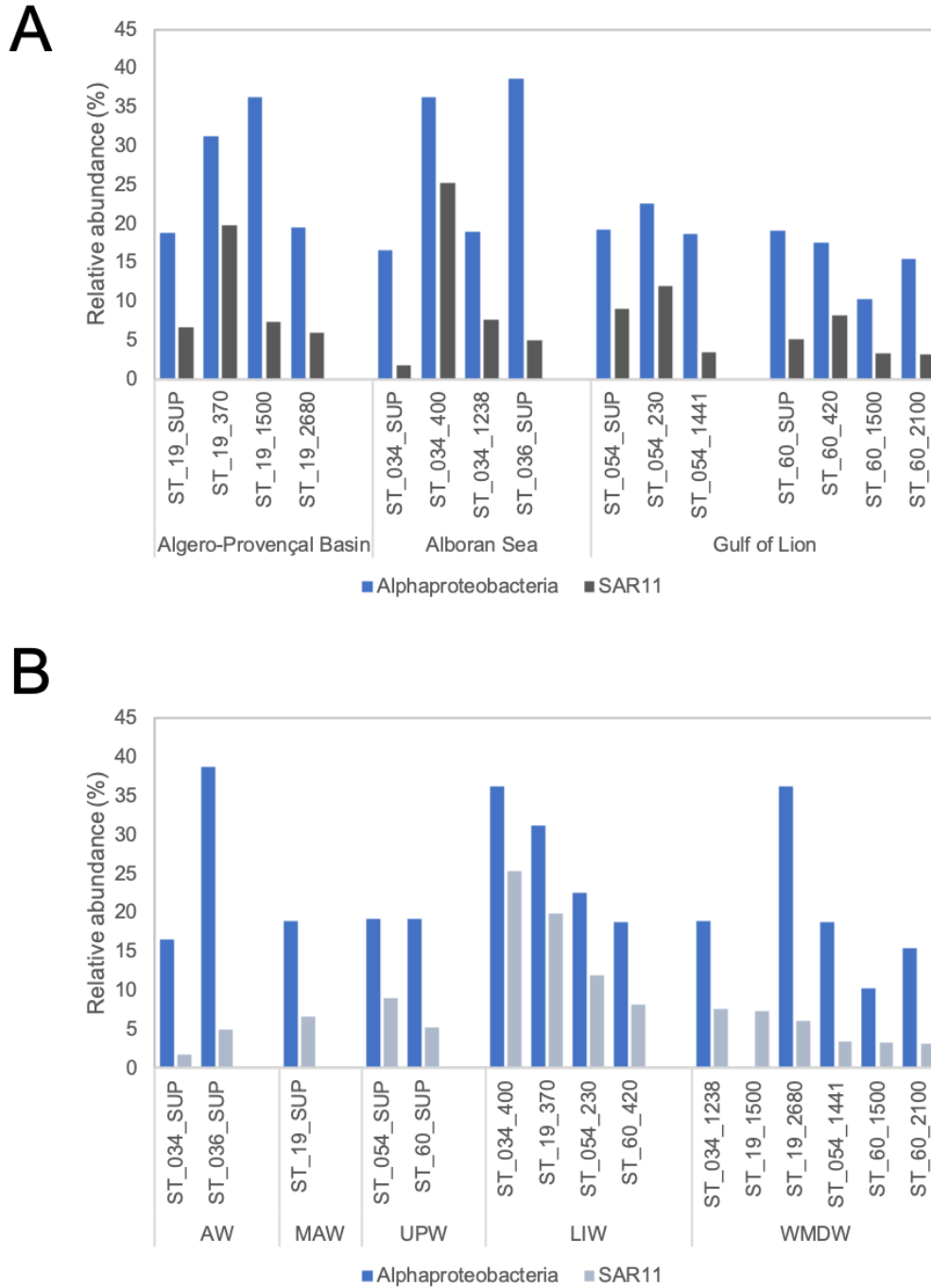
Figure S6. Relative abundances of SAR11 and Alphaproteobacteria reads at each station and area analyzed in our dataset. Panels A and B show data according to area (A) and water mass (B), respectively.
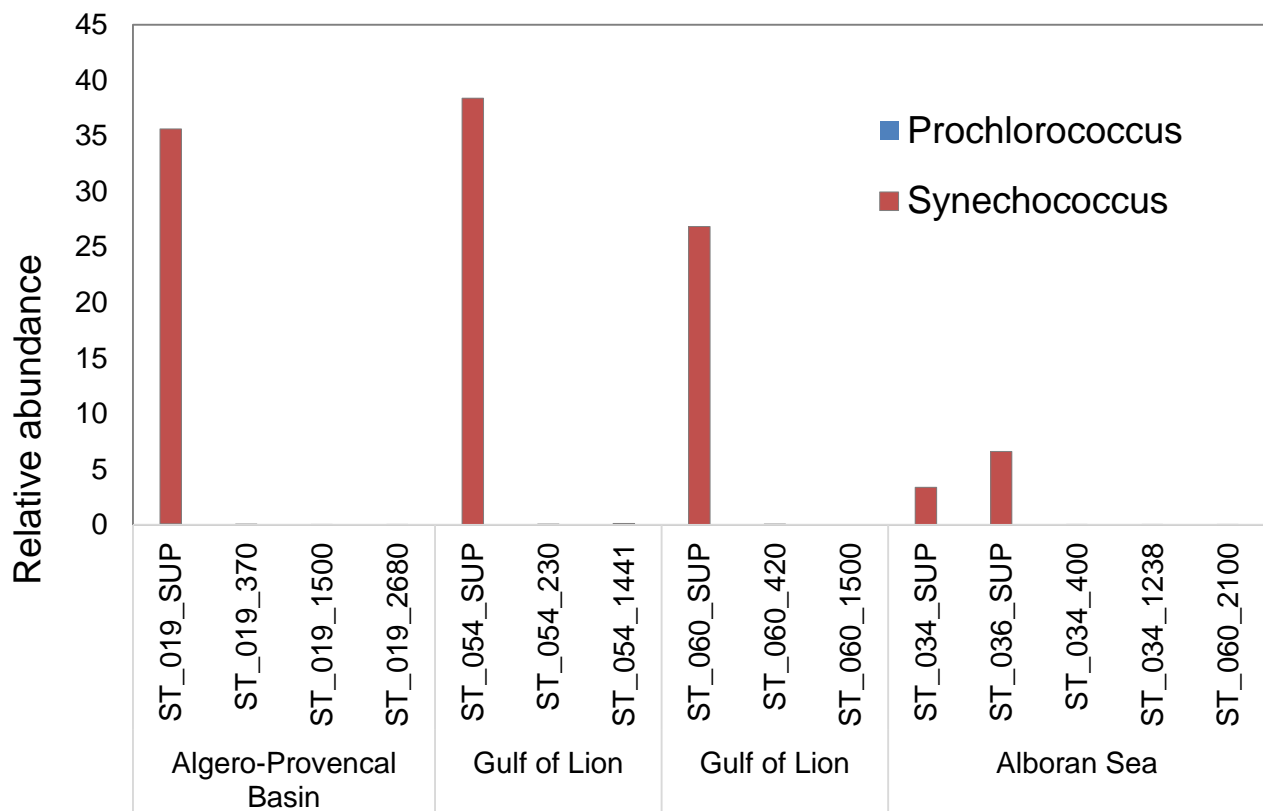
Figure S7. Relative abundances of *Synechococcus* and *Prochlorococcus* at each station and area analyzed in our dataset. *Prochlorococcus* abundances were only detected at stations ST_019_SUP (0.086%) and ST_060_1500 (0.04%); given the very low relative abundance values at these stations, *Prochlorococcus* abundances are not detectable in this plot.
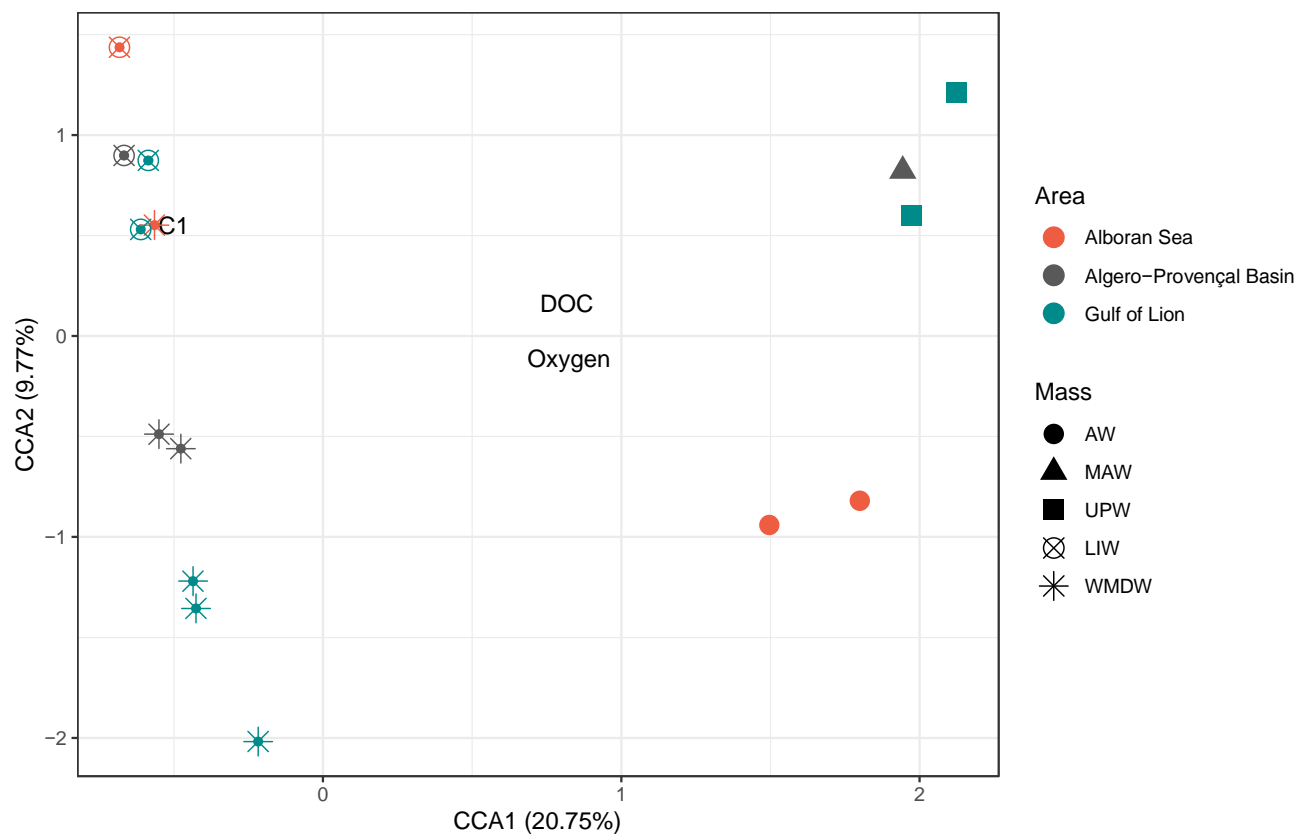
Figure S8. CCA ordination of the PERMANOVA describing the relationship between physicochemical variables and the taxonomic dissimilarity between samples. Vectors represent the relative importance (length) and correlation (angle with axis) between each variable retained in the model and the canonical axes.